

Contract No:

This document was prepared in conjunction with work accomplished under Contract No. DE-AC09-08SR22470 with the U.S. Department of Energy (DOE) Office of Environmental Management (EM).

Disclaimer:

This work was prepared under an agreement with and funded by the U.S. Government. Neither the U. S. Government or its employees, nor any of its contractors, subcontractors or their employees, makes any express or implied:

- 1) warranty or assumes any legal liability for the accuracy, completeness, or for the use or results of such use of any information, product, or process disclosed; or
- 2) representation that such use or results of such use would not infringe privately owned rights; or
- 3) endorsement or recommendation of any specifically identified commercial product, process, or service.

Any views and opinions of authors expressed in this work do not necessarily state or reflect those of the United States Government, or its contractors, or subcontractors.

We put science to work.™



**Savannah River
National Laboratory®**

OPERATED BY SAVANNAH RIVER NUCLEAR SOLUTIONS

A U.S. DEPARTMENT OF ENERGY NATIONAL LABORATORY • SAVANNAH RIVER SITE • AIKEN, SC

Cesium Removal Performance Comparisons of Crystalline Silicotitanate Media Batches with Savannah River Site Waste Simulant

W. D. King

C. A. Nash

K. M. Taylor-Pashow

T. Hang

L. L. Hamm

S. E. Aleman

F. F. Fondeur

May 2020

SRNL-STI-2019-00648, Revision 2

SRNL.DOE.GOV

DISCLAIMER

This work was prepared under an agreement with and funded by the U.S. Government. Neither the U.S. Government or its employees, nor any of its contractors, subcontractors or their employees, makes any express or implied:

1. warranty or assumes any legal liability for the accuracy, completeness, or for the use or results of such use of any information, product, or process disclosed; or
2. representation that such use or results of such use would not infringe privately owned rights; or
3. endorsement or recommendation of any specifically identified commercial product, process, or service.

Any views and opinions of authors expressed in this work do not necessarily state or reflect those of the United States Government, or its contractors, or subcontractors.

Printed in the United States of America

**Prepared for
U.S. Department of Energy**

Keywords: *Salt Processing, Ion Exchange, ZAM, Crystalline Silicotitanate, Tank Closure Cesium Removal, Column, Waste Treatment*

Retention: *Permanent*

Cesium Removal Performance Comparisons of Crystalline Silicotitanate Media Batches with Savannah River Site Waste Simulant

W. D. King
C. A. Nash
K. M. Taylor-Pashow
T. Hang
L. L. Hamm
S. E. Aleman
F. F. Fondeur

May 2020

Prepared for the U.S. Department of Energy under contract number DE-AC09-08SR22470.



REVIEWS AND APPROVALS

SRNL AUTHORS AND REVIEWERS:

W. D. King*, Author/Reviewer, Separation Sciences and Engineering Date

C. A. Nash, Author, Separation Sciences and Engineering Date

T. Hang*, Author/Reviewer, Environmental Modeling Date

L. L. Hamm*, Author/Reviewer, Modeling, Simulation and Analysis Date

S. E. Aleman, Author, Environmental Modeling Date

F. F. Fondeur, Author, Separation Sciences and Engineering Date

K. M. Taylor-Pashow*, Author/Reviewer, Separation Sciences and Engineering Date
Reviewed per E7 2.60

*Review performed by author was of work performed independently by other authors.

APPROVALS:

B. J. Wiedenman, Manager Date
Separation Sciences and Engineering, SRNL

S. D. Fink, Director Date
Chemical Processing Sciences, SRNL

E. J. Freed, SRR Date

EXECUTIVE SUMMARY

The Tank Closure Cesium Removal (TCCR) system uses ion exchange columns filled with Crystalline Silicotitanate (CST) media to process radioactive waste solutions for the removal of Cs-137. The TCCR project is currently focused on dissolving Savannah River Site (SRS) Tank 10H waste (primarily sodium salt cake solids) within the tank followed by at-tank ion exchange column treatment. Plans are underway to prepare and install a second TCCR unit at SRS. Capacity and particle size differences exist between archived (IE-911) and more recently prepared CST media batches (9120-B and 9140-B). Side-by-side comparison testing was performed to evaluate the cesium removal performance of each batch to aid in selecting the preferred CST batch and media characteristics to load into the second TCCR unit. Batch contact equilibrium and flow-through column tests have been conducted with three CST batches using an SRS Average Simulant.

Simulant batch contact equilibrium cesium loading results for the three CST batches (including two lots of one batch) are provided in Table ES-1. The 35 °C data indicates that the archived IE-911 batch has a higher cesium capacity than recently prepared CST media and that the minor TCCR CST 9120-B media lot (2099000035) has similar cesium removal performance to the major TCCR lot (2099000034). Tests conducted at 25 °C for the archived IE-911 CST batch indicated lower cesium removal performance with this simulant batch than was observed recently with a different SRS Average Simulant batch.

A dilution factor (DF) is typically utilized when modeling engineered CST media cesium loading performance to account for mass contributions from the binder material. In cases where CST performance is lower than expected, this factor includes corrections for the binder and for low performance. The ZAM (Zheng, Anthony, and Miller^a) Isotherm Model DF values are provided in Table ES-1 for each simulant batch contact result. DF values near 0.5 were determined for the 9120-B and 9140-B CST batch contact tests while DF values near 0.6 (20% higher) were determined for the tests with IE-911. These dilution factors are lower than recently observed with a different SRS Average Simulant batch (9140-B DF = 0.68; IE-911 DF = 1.0). Based on these results, it appears that some component in the simulant solution used for equilibrium testing may have resulted in reduced cesium loading on the CST media.

Three side-by-side column tests were also conducted at 35 °C using 21.8 g (dehydrated mass basis) CST samples from three of the CST batches and the same Average SRS Simulant used for equilibrium testing. Simulant was pumped through the columns at average flow rates ranging from 3.0-3.4 CST column bed volumes of simulant per hour (corresponds to 1.2 mL/min for each column). Cesium breakthrough profiles plotted on a CST BV basis (BV = media bed volumes of solution processed through column) for each media batch are provided in Figure ES-1. Nearly linear cesium breakthrough profiles were observed for each column under these conditions. Significantly greater (40%) bed volumes of simulant were processed with the archived IE-911 CST prior to reaching the 50% cesium breakthrough point relative to the other two CST batches. Later breakthrough indicates that the IE-911 CST has higher cesium capacity than the other media batches, as was observed in the batch contact equilibrium tests.

VERSE model blind predictions of the cesium column breakthrough profiles for two of CST columns at 35 °C based on previous batch contact equilibrium test results are provided in Figure ES-2 and compared to the experimental data. The experimental batch contact cesium profiles were

^a Z. Zheng, R. G. Anthony, J. E. Miller, "Modeling Multicomponent Ion Exchange Equilibrium Utilizing Hydrous Crystalline Silicotitanates by a Multiple Interactive Ion Exchange Site Model", *Ind. Eng. Chem. Res.*, 1997, 36, 2427.

shifted toward earlier breakthrough and were much less sharp than predicted. The column data for all the CST media tested with this simulant batch indicated both reduced cesium capacity and loading kinetics relative to recent results with these materials and historical data. The impact of particle size differences between the CST batches is difficult to assess due to the poor cesium loading kinetic performance. Based on the results, although IE-911 CST has the smallest average particle diameter, the higher apparent capacity and bed density for this batch have the greatest impact on performance. IE-911 is superior to more recent CST batches with regard to the waste volume processed prior to cesium breakthrough.

The cesium removal performance results are consistent with fouling of the CST media. During the first few hours of column testing, a brown residue was observed to form on the top portion of each CST column (IE-911 column photograph provided in Figure ES-3). Analysis results for the simulant batch utilized for testing were as expected with no indication of impurities. The simulant was filtered twice prior to testing and no solids were visually observed in the liquid entering the column. The poor CST performance with this simulant is not understood.

Report Revision 1 included teabag batch contact test results and column hydraulic test data conducted using the same simulant batch and equipment used for cesium column performance evaluations.

Cesium loadings for the current and newly modified open teabag holder designs are provided in Table ES-2, where higher loadings were observed with the new design, suggesting minor to modest improvement in performance. Due to the high phase ratios used for this testing, final liquid cesium concentrations were essentially the same for each test and were near the initial cesium concentration. Dilution factors versus ZAM calculations show that even with the new holder design, the DFs obtained from the cesium data were found to be 0.29 and 0.26 whereas 0.68 is the traditional expected value for engineered CST. The low DFs observed were likely related to the simulant instability with regard to precipitation which was discovered at a later date and is discussed in this report revision. Presumably, higher phase ratio testing with no agitation is more susceptible to CST fouling effects than traditional batch contact tests. Interestingly, the respective DFs for potassium, found later in this report, are close to unity.

Column frictional pressure drop data under dynamic flow conditions for the three columns used for cesium performance testing is provided in Figure ES-4. A linear pressure drop dependence was observed versus liquid flow rate for each column up to the highest superficial velocity evaluated of 14 cm/min (near the TCCR facility operating superficial velocity) indicating laminar flow conditions. Trends in the frictional pressure drop data were consistent with the volume-based particle diameters with lower pressure drops being observed for larger mean particle diameters. At a given flow rate, the pressure drop observed for IE-911 CST was 19% higher than the pressure drop observed for the TCCR 9120-B CST media (linear regression slope of 0.10 for IE-911 versus 0.088 for 9120-B). The pressure drop observed for 9140-B CST was 28% lower than the pressure drop observed for the TCCR 9120-B CST media (linear regression slope of 0.063 for 9140-B versus 0.088 for 9120-B). Relative to IE-911 CST, 16 and 39% lower pressure drops, respectively, were observed for 9120-B and 9140-B CST samples. The mobile fluid bed volume fractions determined separately for each CST batch (IE-911 – 18.0%; 9120-B – 22.9%, and 9140-B – 27.4%) are representative of the packed bed porosity and correlate better to the trends in the hydraulic data than the mean particle diameter values.

Report revision 2 includes additional analysis data on the simulant, the CST media from the columns, the solids isolated from the simulant drum and columns, and CST blank samples. This additional data was needed to explain the poor cesium column loading kinetics observed. The primary chemical components of the precipitated solids isolated from the simulant drum and the CST columns are provided in Table ES-3. An XRD scan of the drum solids is provided in Figure ES-5. Based on the additional analysis results, supersaturated concentrations of some metal species are believed to have existed in the simulant solution despite the fact that the simulant had been aged for several weeks prior to testing. This resulted in the co-precipitation of calcium, aluminum, magnesium, manganese, and iron species from solution. Except for aluminum, the metals were present at concentrations below analytical detection limits in the column simulant feed. These species included calcium carbonate and possibly magnesium carbonate, which have retrograde solubility and would be expected to have precipitated in the column head when the temperature was increased from ambient to 35 °C.

Table ES-1. Average Cesium Equilibrium Distribution Coefficients (K_d), % Removal, Loading and Calculated ZAM DFs for Various CST Batches with SRS Average Simulant.

CST Batch/Sample ^a	Temperature (°C)	Average Cs ⁺ K_d (mL/g) ^c	Cs ⁺ K_d %RSD	Cs ⁺ % Removal	mmol Cs ⁺ /g CST ^c	ZAM Dilution Factor (DF) ^e
Archived VP IE-911	25 ^d	1432	0.7	94.0	3.91E-03	0.617
	35	1057	6.2	91.8	3.79E-03	0.590
FP 9120-B (Lot 2099000034)	35	907	2.7	90.1	3.89E-03	0.507
FP 9120-B (Lot 2099000035) ^b		892	5.0	89.8	3.96E-03	0.499
VP 9140-B		874	1.9	89.9	3.82E-03	0.489

^a FP = field-pretreated, VP = vendor pretreated

^b Lot #2099000035 (minor TCCR column CST batch)

^c dry, engineered CST mass basis (f-factor corrected based on mass loss up 410 °C)

^d Note: An oven thermocouple error discovered at test completion did not allow confirmation that the temperature throughout testing was at the target value.

^e Correction factor applied to model predictions to account for CST mass contributions from binder material.

Table ES-2. Comparisons of Teabag CST Loadings and Liquid Cesium Concentrations for Current and Modified Open Holder Designs

Test	Teabag Holder Design	Final Liquid Cs ⁺ (M)	CST Loading, Cs ⁺ mmol/g ^a	ZAM Dilution Factor
A	Current	4.27E-05	4.91E-03 ^b	0.063 ^b
	Modified Open	4.27E-05	2.28E-02	0.29
B	Current	4.23E-05	1.68E-02	0.21
	Modified Open	4.23E-05	2.02E-02	0.26

^a dry, engineered CST mass basis

^b the lower loading and DF for this sample versus the Test B replicate are not understood

Table ES-3. Selected Characterization Data on Digested Solids Isolated from the CST Columns and Simulant Drum After Test Completion.

Metal	Solids from Column A (IE-911)	Solids from Column B (9120-B)	Solids from Column C (9140-B)	Simulant Drum Solids
	µg/g solid (hydration level unknown)			
Al	2140	3230	4890	34100
Ca	<47.4	828	72.5	35000
Fe	107	168	124	993
Mg	650	1335	802	2690
Mn	231	373	265	918

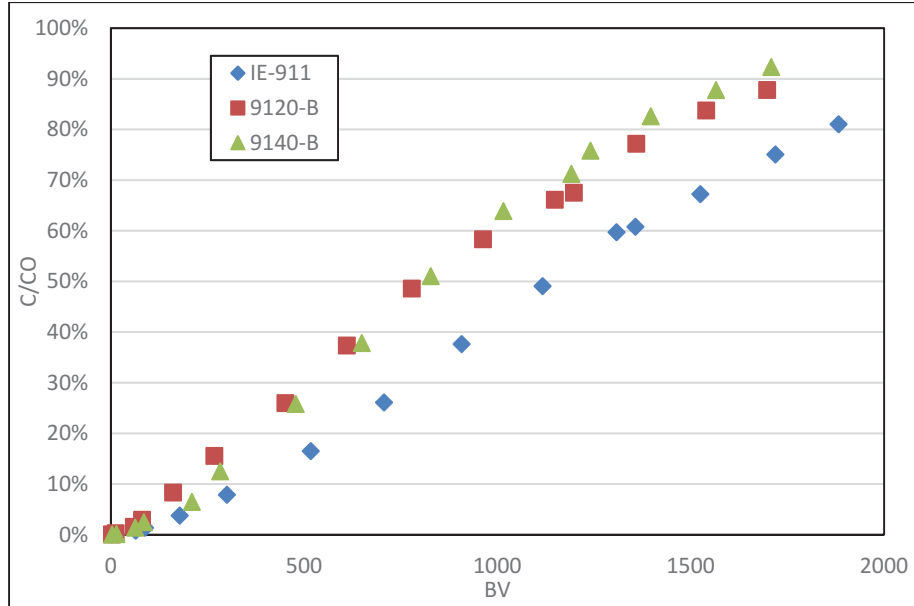


Figure ES-1. Cesium Column Instantaneous Breakthrough Profiles for Three CST Media Batches at 35 °C at Flow Rates of 3.0-3.4 BV/hr.

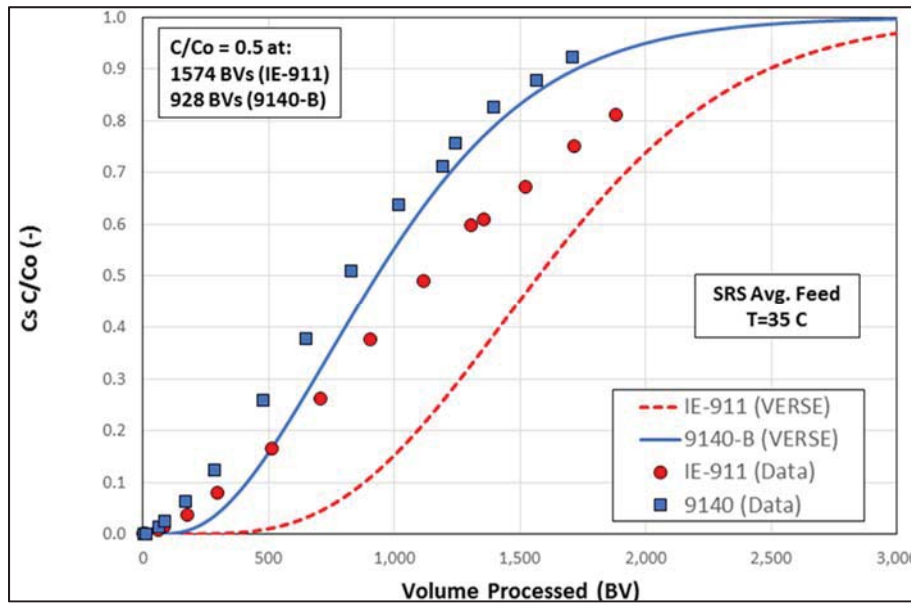


Figure ES-2. VERSE Model Predictions Versus Measured Cesium Instantaneous Breakthrough Profiles for IE-911 (DF = 1.0 and $\tau = 4.0$) and 9140-B CST (DF = 0.68 and $\tau = 4.0$) at 35 °C at the Average Flow Rates Used for Testing (expected performance based on historical testing).

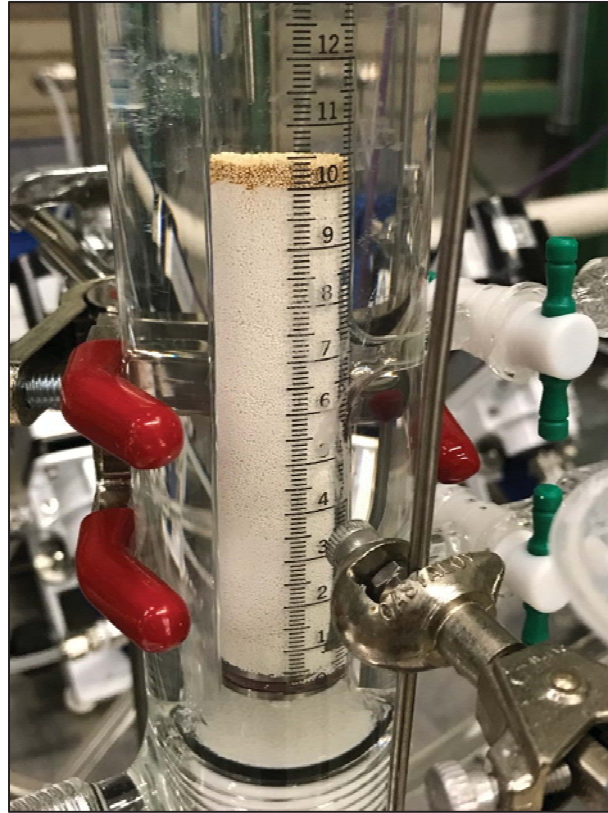


Figure ES-3. Brown Residue Observed on the Top of the IE-911 CST Column During Testing.

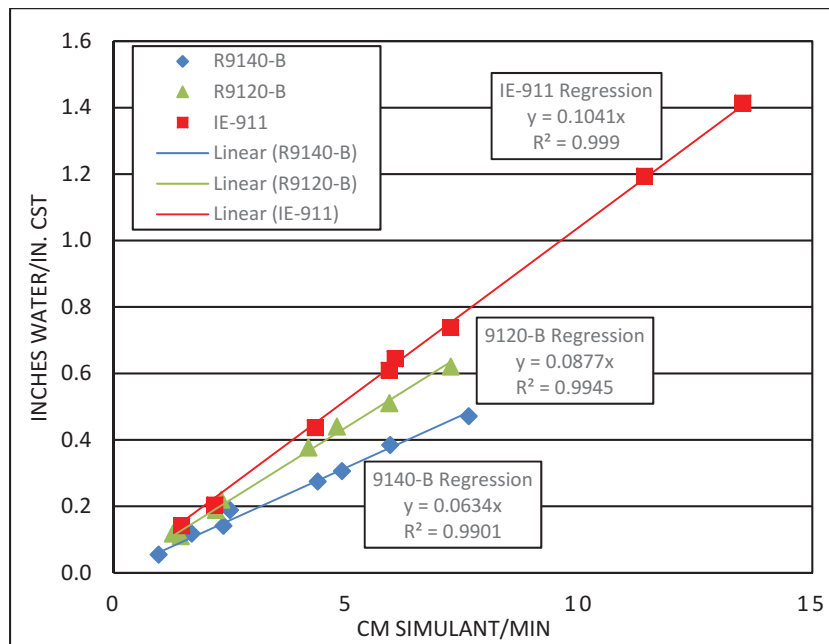


Figure ES-4. Column Frictional Pressure Drop Data for Three CST Batches in SRS Average Simulant at 24 °C Following Cesium Performance Testing.

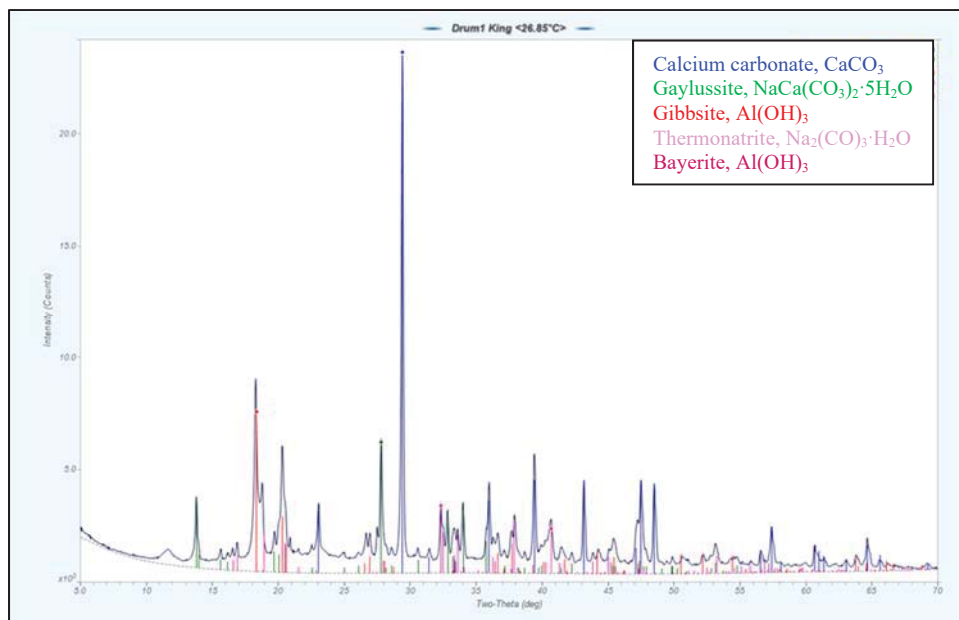


Figure ES-5. X-Ray Diffraction Scan of the Simulant Drum Solids.

TABLE OF CONTENTS

LIST OF FIGURES	xiv
1.0 Introduction.....	1
1.1 Quality Assurance	1
2.0 Experimental Methods and Modeling Approach.....	2
2.1 CST Media Batches and Pretreatment.....	2
2.2 CST Water Content Determination	3
2.3 SRS Average Simulant Preparation	3
2.4 CST Batch Contact Testing.....	4
2.5 Teabag Batch Contact Testing	5
2.6 Column Testing.....	8
2.7 ZAM Isotherm and VERSE Column Model Calculations	11
2.8 Column Hydraulic Testing	12
2.9 CST Particle Size Determination	14
3.0 Results and Discussion	16
3.1 CST Batch Contact Equilibrium Test Results.....	16
3.2 ZAM Isotherm Modeling of the Batch Contact Data.....	16
3.3 CST Column Results.....	17
3.4 VERSE Column Modeling.....	22
3.6 Teabag Batch Contact Testing	28
3.7 Additional Characterization Data Following Test Completion.....	30
4.0 Conclusions.....	41
5.0 Recommendations and Path Forward	42
6.0 References.....	43
Appendix A . TGA Data	A-1
Appendix B . ZAM β Factor Temperature Dependence for SRS Average Simulant.	B-1
Appendix C . Teabag CST Digestion Data.	C-1

LIST OF TABLES

Table 2-1. CST F-factor Data.	3
Table 2-2. Target SRS Average Simulant Composition.	4
Table 2-3. CST and SRS Average Simulant Masses Used for Cesium Batch Contact Equilibrium Testing. 5	
Table 2-4. Teabag Hardware and CST Masses.	6
Table 2-5. Masses, Bed Densities, and Dimensions for CST Columns.	10
Table 2-6. Simulant Volumes Processed and Flow Rates for CST Column Tests.	10
Table 2-7. 9120-B Lot 2099000035 CST Vendor Sieve Data.	14
Table 2-8. 9140-B Lot 2002009604 CST Vendor Sieve Data.	14
Table 3-1. Cesium Equilibrium Distribution Coefficients, % Removal, Loading and Calculated ZAM DFs for Various CST Batches with the SRS Average Simulant Batch Used for Column Testing.	17
Table 3-2. Frictional Pressure Drop Data for CST Columns.	27
Table 3-3. Teabag Rinse Liquid Analysis.	29
Table 3-4. CST Cesium Loading and Liquid Cesium Concentrations.	30
Table 3-5. CST Potassium Loading and Liquid Potassium Concentration.	30
Table 3-6. Additional Simulant Feed and Column Effluent Analysis.	31
Table 3-7. ICP-ES and ICP-MS Data on Digested CST Column Sub-Samples After Cesium Performance and Hydraulic Test Completion.	34
Table 3-8. TCCR CST Digestion Standards Average ICP-MS and ICP-ES Data.	35
Table 3-9. Metal Loading Data on the CST Column Sub-Samples.	36
Table 3-10. ICP-ES and ICP-MS Data on Digested Solids Isolated from the CST Columns and Simulant Drum After Test Completion.	38
Table 3-11. Microtrac Particle Size Distribution Data for CST Column Sub-Samples.	39
Table 3-12. Particle Size Distribution and Drainable Void Data for CST Production Batches and Column Sub-Samples.	39

LIST OF FIGURES

Figure 2-1. Current Teabag Holder Design Utilized Prior to TCCR Processing.....	6
Figure 2-2. Newly Modified “Open” Teabag Holder Design.....	7
Figure 2-3. Modified Stainless Steel Dip Vial for CST Teabag Batch Contacts.....	7
Figure 2-4. CST Teabag Hardware.....	8
Figure 2-5. Ion Exchange Column Design.....	9
Figure 2-6. Flow Rate Data for Each Column.....	11
Figure 2-7. Glass Manometer Used for Column Hydraulic Testing.....	13
Figure 2-8. Cumulative Particle Diameter Distribution Function for CST Batch 9120-B Lot 2099000035 Based on the Vendor Sieve Data in Table 2-7.....	15
Figure 2-9. Cumulative Particle Diameter Distribution Function for CST Batch 9140-B Lot 2002009604 Based on the Vendor Sieve Data in Table 2-8.....	15
Figure 3-1. ZAM Isotherm Predictions Versus Observed Batch Contact Data.....	18
Figure 3-2. Brown Residue Observed on the Top of the IE-911 CST Column During Testing.....	18
Figure 3-3. Brown Residue Observed on the Top of the 9120-B CST Column During Testing.....	19
Figure 3-4. Brown Residue Observed on the Top of the 9140-B CST Column During Testing.....	19
Figure 3-5. Cesium Column Instantaneous Breakthrough Profiles Versus Simulant BVs Processed for Three CST Media Batches at 35 °C at Flow Rates of 3.0-3.4 BV/hr.....	20
Figure 3-6. Cesium Column Instantaneous Breakthrough Profiles Versus Cumulative Simulant Volume for Three CST Media Batches at 35 °C at Flow Rates of 3.0-3.4 BV/hr.....	21
Figure 3-7. Initial Cesium Column Instantaneous Breakthrough Profiles for Three CST Media Batches at 35 °C at Flow Rates of 3.0-3.4 BV/hr.....	21
Figure 3-8. VERSE Model Predictions Versus Instantaneous Measured Cesium Breakthrough Profiles for IE-911 and 9140-B CST at 35 °C at the Average Flow Rates Used for Testing of 3.0-3.4 BV/hr.....	23
Figure 3-9. Semi-log Plot of VERSE Model Predictions Versus Instantaneous Measured Cesium Breakthrough Profiles for IE-911 and 9140-B CST at 35 °C at the Average Flow Rates Used for Testing of 3.0-3.4 BV/hr.....	23
Figure 3-10. VERSE Model Predictions Versus Measured Cesium Instantaneous Breakthrough Profiles for IE-911 and 9140-B CST at 35 °C at the Average Flow Rates Used for Testing.....	24
Figure 3-11. VERSE Model Predictions Versus Measured Cesium Instantaneous Breakthrough Profiles for IE-911 and 9140-B CST at 35 °C at the Average Flow Rates Used for Testing.....	24
Figure 3-12. Frictional Pressure Drop versus Flow Rate Profiles for CST Columns Measured in SRS Average Simulant at 23-30 °C.....	26

Figure 3-13. CST Samples Removed from 9120-B CST Column in ~1 cm Segments.	33
Figure 3-14. CST Samples from Upper Portion of Each Column and the 2 nd and Bottom Portions of Column B after Isolation and Washing to Remove Precipitates.	33
Figure 3-15. Brown Solids Isolated from the CST Columns and the Simulant Drum.....	33
Figure 3-16. X-Ray Diffraction Scan of the Simulant Drum Solids.....	39
Figure 3-17. Volume-Based Microtrac Particle Size Distribution for the IE-911 CST Sub-sample from Column A.	40
Figure 3-18. Volume-Based Microtrac Particle Size Distribution for the 9120-B CST Sub-sample from Column B.....	40
Figure 3-19. Volume-Based Microtrac Particle Size Distribution for the 9140-B CST Sub-sample from Column C.....	40

LIST OF ABBREVIATIONS

BV	Ion Exchange Column Bed Volumes
CST	Crystalline Silicotitanate
DF	CST mass Dilution Factor
DOE	Department of Energy
dpm	disintegrations per minute
ELN	Electronic Laboratory Notebook
g	gram
ICP-ES	Inductively Coupled Plasma - Emission Spectroscopy
ICP-MS	Inductively Coupled Plasma - Mass Spectroscopy
ID	Inside diameter
K _d	Distribution Coefficient
LC	Liquid Chromatography
mL	milliliter
OD	outside diameter
PVDF	polyvinyl difluoride
rpm	revolutions per minute
SRNL	Savannah River National Laboratory
SRR	Savannah River Remediation
SRS	Savannah River Site
SS	stainless steel
TCCR	Tank Closure Cesium Removal
TGA	Thermal Gravimetric Analysis
TTQAP	Task Technical and Quality Assurance Plan
TTR	Technical Task Request
VERSE	VERsatile Reaction SEparation chromatography model
ZAM	Zheng, Anthony, and Miller Isotherm Model
β	ZAM Beta Parameter
τ	tortuosity factor

1.0 Introduction

Near the beginning of calendar year 2019, Savannah River Remediation (SRR) deployed the Tank Closure Cesium Removal (TCCR) system using an ion exchange process to remove radioactive cesium from waste supernate. In TCCR, radioactive salt solution is filtered and then passed through ion exchange columns containing crystalline silicotitanate (CST) media, commercially known as UOP IONSIV™ 9120-B^a (formerly called IE-911), to remove cesium. The TCCR project is currently focused on dissolving Savannah River Site (SRS) Tank 10H waste (primarily sodium saltcake solids) within the tank followed by at-tank (or near-tank) ion exchange column treatment. Four TCCR columns were prepared, loaded with CST, and installed at SRS. Previous batch contact tests with SRS simulant indicated that IE-911 CST media has a higher cesium capacity than the recent CST batches prepared (9120-B and 9140-B). The higher capacity is reflected in the fact that a CST binder dilution factor (DF; factor accounting for mass contributions from binder material or for low performance) of 1.0 was required for IE-911 to match the experimental data to model predictions [1] while a dilution factor near 0.7 was required for 9120-B CST [2]. Based on these results, it was anticipated that IE-911 column performance would exceed that of the other batches by about 30%. Batch contact equilibrium and column testing were conducted with various CST media batches and SRS Average simulant to evaluate and compare cesium removal performance for each batch.

SRR also requested CST cesium loading kinetics testing under unagitated conditions using a CST sample holder referred to as a “teabag”. This testing is intended to measure the extent of cesium loading on CST under the high liquid:solid phase ratio conditions that should exist during teabag deployment in a waste tank. The current work documents testing with a new, open style of holder for the “teabag” batch contact device. The device holds a measured amount (~0.1 grams) of pretreated CST between stainless steel screens. Immersion of the device allows free contact of the CST beads with surrounding liquid. This work involved teabag contact with non-radioactive, cesium-bearing “SRS Average” simulant under unstirred conditions. This information builds upon testing which had been performed and reported several months ago [3]. The current work compares the performance of two separate designs of teabag unit holders (current and new open design) under ambient conditions. The batch contact tests were conducted for 10 days with each teabag unit holder being tested in duplicate giving a total of four tests.

Column frictional pressure drop tests under dynamic flow conditions were also conducted on the packed CST columns from three media batches which were previously used for column performance testing. The pressure drop data will impact the media specifications for future CST procurements.

After test completion, additional analysis was conducted on the simulant, the CST media from the columns, the solids isolated from the simulant drum and columns, and CST blank samples to explain the poor cesium column loading kinetics observed.

1.1 Quality Assurance

Requirements for performing reviews of technical reports and the extent of review are established in Manual E7, Procedure 2.60. SRNL documents the extent and type of review using the SRNL Technical Report Design Checklist contained in WSRC-IM-2002-00011, Rev. 2. The work was performed following the applicable TTQAP, Technical Task and Quality Assurance Plan [4]. The

^a IONSIV is a trademark of Honeywell UOP, Des Plaines, IL, U.S.A.

Technical Task Request (TTR) associated with this work [5] indicates that portions of this work are Safety Significant, but that the testing reported herein and the supporting modeling are for Production Support rather than technical baseline and are not Safety Significant (see section entitled “Clarification of Safety Significant Tasks”). The software packages used as part of this work scope must comply with 1Q, QAP 20-1 Software Quality Assurance, E7, Section 5.0 and Software Engineering and Control, Applicable provisions of Section 5.4, Procedure 2.31, E7 Manual. Column and standard batch contact data are recorded in the Electronic Laboratory Notebook (ELN) system as notebook/experiment number A2341-00117-12. A spreadsheet containing analytical data and batch contact and column performance calculations is included in this ELN experiment. Experimental details for the teabag tests are contained in Research and Development (R&D) Directions. Completed R&D Directions are stored in ELN experiment T7692-00094-07.

The ZAM Isotherm Model code is purchased commercial software developed at Texas A&M University by Z. Zheng, R. G. Anthony, and J. E. Miller designed to simulate ion-exchange equilibria of electrolytic solutions and CST solids. The ZAM model is currently classified as Level D software [6] and ZAM calculations meet the Production Support needs specified for this task in the TTR. The functional requirements placed on ZAM were verified and validated [7].

The VERSE-LC column model code is purchased software for the prediction of mass transfer and retention of sorbing species through liquid chromatography columns. Prior to applying VERSE-LC to the ion exchange modeling a verification process was completed and the results of that effort were reported by Hamm et al. [8]. The verification process ensures that the installed Windows version of VERSE-LC (i.e., version 7.80) was capable of adequately solving the above-mentioned governing equations and provided guidelines on how to accurately use the VERSE-LC code (e.g., mesh refinement requirements and input/output options). For all column simulations, numerical errors associated with the results of VERSE-LC should be very small when compared to the uncertainties associated with various model input parameters (bed density, particle size, pore diffusion, etc.). VERSE-LC was classified as Level D [9] and VERSE calculations meet the Production Support needs specified for this task in the TTR.

2.0 Experimental Methods and Modeling Approach

2.1 CST Media Batches and Pretreatment

The following CST ion exchange media batches were used for this testing:

- IE-911 Lot #2081000056, Mat. #80562-556p, and drum #36232-1-5,
- 9120-B Lots 2099000034 (Material #8103701-556, Sub-sample from CUA #125953-A) and 2099000035, and
- 9140-B Lot 2002009604.

The TCCR column CST media from production batch IONSIV 9120-B and Lots 2099000034 (major TCCR media lot) and 2099000035 (minor TCCR lot) were pretreated as described previously [10] using an abbreviated field methodology with lower volumes of 3 M NaOH and longer contact times than standard laboratory pretreatment methods used historically [2]. The IE-911 and 9140-B CST batches were pretreated by the vendor prior to shipment and were used as-received. The 9120-B and 9140-B are recently prepared CST batches while the IE-911 CST media has been stored at SRS for nearly two decades. Recent batch contact testing with the IE-911 CST

and SRS Average simulant confirmed that the cesium removal performance of this media had not changed significantly during storage [1]. Batch contact testing with the 9120-B Lot #2099000034 CST and SRS Average Simulant was also conducted recently which indicated that the media performed comparably to past results, though with a binder dilution less than 1 [2].

2.2 CST Water Content Determination

Thermal Gravimetric Analysis (TGA) was conducted on each CST batch in duplicate to determine the water content. The thermal analysis involved heating sub-samples of CST at a rate of 5 °C per minute to 400 °C and holding the sample at that temperature for 240 minutes followed by a second heating period up to 700 °C. The total mass loss was determined as the sum of several successive mass losses believed to be associated with both physisorbed and chemisorbed water loss. Mass loss data for each CST sample up to 410 °C is summarized and average F-factor (mass correction factor for water content) values are provided in Table 2-1. Mass loss profiles collected for each CST sample during TGA analyses are provided in Appendix A.

Table 2-1. CST F-factor (Dry Mass Correction Factor) Data.

CST Batch/Sample ^a	Sample	(Wt. %)			F-factor ^b
		Mass Loss at 410 °C	Average Mass Loss	Mass Loss %RSD	
FP 9120-B Lot 2099000034	A	17.848	17.912	0.5%	0.821
	B	17.976			
FP 9120-B Lot 2099000035	A	18.726	19.029	2.3%	0.810
	B	19.332			
Archived VP IE-911	A	16.167	16.123	0.4%	0.839
	B	16.079			
VP 9140-B	A	16.194	16.158	0.3%	0.838
	B	16.122			

^a FP = field-pretreated, VP = vendor pretreated

^b mass correction factor for water content

2.3 SRS Average Simulant Preparation

Thirty-five (35) gallons of Average SRS Simulant were prepared with the target composition provided in Table 2-2 following the recipe reported by Walker [11]. This simulant was developed to represent an average SRS waste supernate liquid and this solution composition has been used in the past for CST performance evaluations. The simulant contains 5.6 M Na⁺ and 1.9 M free OH⁻, with nitrate and nitrite anions being the next most concentrated anions present. Cesium nitrate was added to give a final total cesium concentration near 6 mg/L. The large-scale simulant was prepared with 34 wt % aluminum nitrate solution rather than using the solid reagent specified in the recipe. Preliminary small-scale simulant batches were prepared using aluminum nitrate solution and solid reagent, which were each confirmed to contain the target aluminum concentration. Silicon oxide reagent was omitted from the recipe since previous testing has indicated that silicon does not remain in solution. The simulant was filtered twice through a 1.0-µm filter. The measured simulant density was 1.253 g/mL at ambient temperature (21 °C).

Simulant analysis results are also provided in Table 2-2. Results were within 10% of the target values for most species. The fluoride ion concentration was only 53% of the target value and the oxalate ion concentration was only 72% of the target. These are minor components were not expected to influence cesium removal significantly. The calcium concentration was $<3\text{E-}5$ M and the iron concentration was $<2\text{E-}4$ M. Digestion of CST samples contacted with waste supernate samples has indicated calcium and iron uptake by CST [12].

Table 2-2. Target SRS Average Simulant Composition.

Component	Molarity		Measured/Target
	Target	Measured	
Na ⁺	5.60	5.55	0.99
K ⁺	0.015	0.015	1.01
OH ⁻	1.91	1.82	0.95
NO ₃ ⁻	2.14	2.13	0.99
NO ₂ ⁻	0.52	0.51	0.99
AlO ₂ ⁻	0.31	0.33	1.08
CO ₃ ²⁻	0.16	0.17	1.04
SO ₄ ²⁻	0.15	0.15	0.99
Cl ⁻	0.025	0.024	0.97
F ⁻	0.032	0.017	0.53
PO ₄ ³⁻	0.01	0.007	0.71
P (ICP-ES)	---	0.010	0.96
C ₂ O ₄ ²⁻	0.008	0.006	0.72
MoO ₄ ²⁻	0.0002	<0.0002	---
Cs ⁺	4.5E-5	4.4E-05	0.98

2.4 CST Batch Contact Testing

Duplicate or triplicate 10 mL sub-samples of SRS Average Simulant were filtered (0.2 μm PVDF) and used for equilibrium batch contact testing with ~0.12 g samples (~0.1 g after water content correction) of CST media. Innova incubated shaker ovens were used for batch contact testing using an agitation rate of 150 rpm. The supernate and CST test samples were placed in 60 mL polyethylene bottles, transferred to the shaker oven, and continuously agitated for 4-7 contact days at 25 or 35 °C. A total of 4 contact days was used for the 35 °C tests with IE-911, while the other tests involved 6-7 days of contact. The oven display temperature was manually monitored and recorded periodically throughout testing and was checked with a calibrated thermocouple at test completion and confirmed to be within 1 °C of the target value. At test completion, individual samples were removed from the shaker, filtered through 0.2-μm syringe filters, and submitted for cesium analysis by ICP-MS with no dilution. Separate filtered simulant sub-samples were also placed in 60 mL bottles, agitated in the shaker oven alongside the batch contact test samples (no CST contact), filtered again, and submitted for analysis. The CST and simulant supernate masses for individual samples during equilibrium batch contact testing are provided in Table 2-3. During the 25 °C batch contact tests an oven thermocouple error was discovered at test completion which

did not allow confirmation that the temperature throughout testing was at the target value. Although it is believed that the temperature was constant, this cannot be confirmed.

Table 2-3. CST and SRS Average Simulant Masses Used for Cesium Batch Contact Equilibrium Testing.

CST Batch ^a	Temperature (°C)	CST (g) ^b	SRS Average Simulant (g)	SRS Average Simulant (mL) ^c
FP 9120-B Lot 2099000034	35	0.1229	12.5500	10.0
		0.1229	12.5592	10.0
FP 9120-B Lot 2099000034		0.1215	12.5598	10.0
0.1221		12.5481	10.0	
Archived VP IE-911	25	0.1237	12.5279	10.0
		0.1364	12.5236	10.0
	35	0.1284	12.7800	10.2
		0.1250	12.5628	10.0
VP 9140-B	35	0.1304	12.5571	10.0
		0.1222	12.5514	10.0
		0.1220	12.5712	10.0

^a FP = field-pretreated, VP = vendor pretreated

^b hydrated CST reference state masses; multiply by appropriate f-factors to correct to dry state mass basis

^c simulant volumes calculated using the measured density of 1.253 g/mL

2.5 Teabag Batch Contact Testing

Portions of the 35-gallon simulant batch were used for “teabag” batch contact testing prior to the initiation of CST column testing. “Field pretreated” 9120-B CST Lot 2099000034 was used for teabag testing. This material is from the same batch of pretreated CST used to load teabag units for deployment in Tank 10H. The primary purpose of this teabag testing was to compare the performance of the current teabag holder with a new and more open design. A pair of photographs are provided in Figure 2-1 showing the current teabag holder design. The device was fabricated from perforated stainless steel (SS) sheet. The modified, open holder design is shown in Figure 2-2. This device was welded together from 1/8” rods, two washers (bottom and middle) and a top ring formed by a thin slice of tubing. All component parts are 304 stainless steel. Both the current and new holders are 1.5” outside diameter (OD) and narrowly fit into the sample vial shown in Figure 2-3. The bottom washer of the new holder is 1.5” in OD and so must be drilled at the edge so that the rods can be attached by welding. The middle washer has an additional modification where the inside diameter (ID) is drilled to 1.112”. That increased diameter fits the round part of the Swagelok™ nut of the teabag, below the hexagonal nut. The teabag easily fits into the holder by passing through the upper ring. The components of a disassembled teabag are shown in Figure 2-4. The teabag can be loaded with CST by placing one of the screens into the Swagelok™ nut to the right of the picture, adding pre-weighed ion exchange media, inserting the other screen to sandwich the media between the screens, and then adding the Swagelok™ ferrules. All these components are held together by attaching the nut cap shown to the left of the photograph and

tightening the nuts by hand. The cap was modified to give an ID of 0.75". Diagrams of the hardware are found in the procedure for loading the teabag units [13].

In the current work, the hardware parts were weighed prior to assembly. The mass of CST resin was also recorded in each case. Table 2-4 provides the hardware masses before and after loading/assembly, and the mass of CST along with the weight gain of the completed holder. Masses agreed within 0.5 mg, showing that the CST being used here was effectively loaded into the units without significant particle loss or fines generation.

Table 2-4. Teabag Hardware and CST Masses.

Test (Holder Design)	Empty Hardware Including 2 Screens (g)	Directly Measured CST (g)	Loaded Hardware + CST (g)	Indirectly Measured CST; Loaded Minus Empty Hardware (g)	Mass Difference Between CST Measurement Methods (mg)
A (Current)	80.4303	0.1000	80.5302	0.0999	0.1
A (New open)	83.0597	0.0998	83.1595	0.0998	0.0
B (Current)	83.0715	0.1000	83.1713	0.0998	0.2
B (New open)	80.4434	0.1001	80.5430	0.0996	0.5

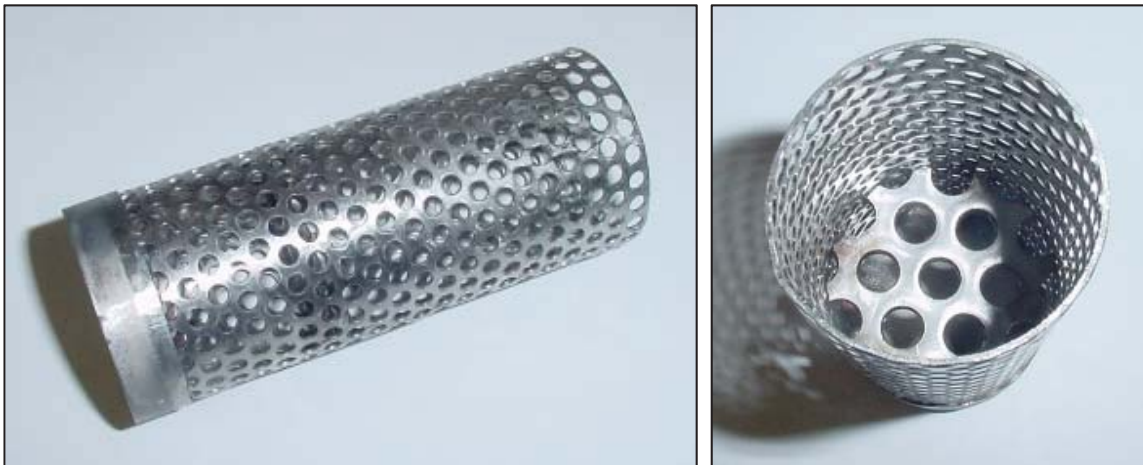


Figure 2-1. Current Teabag Holder Design Utilized Prior to TCCR Processing.



Figure 2-2. Newly Modified “Open” Teabag Holder Design.



Figure 2-3. Modified Stainless Steel Dip Vial for CST Teabag Batch Contacts.



Figure 2-4. CST Teabag Hardware.

2.6 Column Testing

Three customized borosilicate glass columns were prepared in the SRNL glass shop for evaluating the CST media. The column design is provided in Figure 2-5. The columns were prepared from 1.75 cm ID glass tubing and contained outer glass jackets for temperature control. A recirculating unit was used to pump warm water through the outer jacket to maintain the column temperature at the target value of 35 °C. The CST media was wetted in 3 M NaOH solution and the resulting slurries were gently agitated to remove air bubbles. The slurries were quantitatively transferred into the columns in multiple small portions, taking care to minimize the liquid height and CST settling distance to avoid bed segregation. Calibrated thermocouples were inserted into the liquid headspace above the CST beds to monitor the temperature. The temperature was generally recorded daily during effluent sub-sampling events (average and %RSD temperature data: Column A – 34.9 °C, 0.3%; Column B – 35.0 °C, 0.2%; Column C – 34.9 °C, 0.2%). 100 mesh screens were placed along one side of the packed CST beds to prevent transfer of CST beads into the pressure taps to be used in subsequent pressure drop testing. Screens (100 mesh) were also utilized to support the bottoms of the packed CST beds within the columns. Approximately 1 mm glass beads were packed in the void space below the screens to promote consistent fluid flow through the bottom of the column and to minimize the mixing volume below the column upstream of the sub-sampling location. The columns were designed to be operated without pressurized heads. Sufficient headspace was available above the packed CST beds to create the liquid head height needed to transfer solution through the bed at the target flow rate. The column heads were open to the atmosphere throughout testing and the liquid levels in the columns generally remained constant during testing.

The CST masses and the bed dimensions for each column are provided in Table 2-5. Stainless steel tubing with a nominal 1/8-inch outside diameter (not shown) was attached to the bottoms of the columns and fashioned into a loop which extended up above the tops of the CST beds. This configuration prevented the columns from draining when flow was interrupted, but also allowed sub-sampling to be conducted without flow interruption. Approximately 3 mL effluent sub-

samples were collected for 2.5 minutes on a daily frequency during testing and submitted for cesium analysis by ICP-MS. As a result, the cesium breakthrough profiles represent the

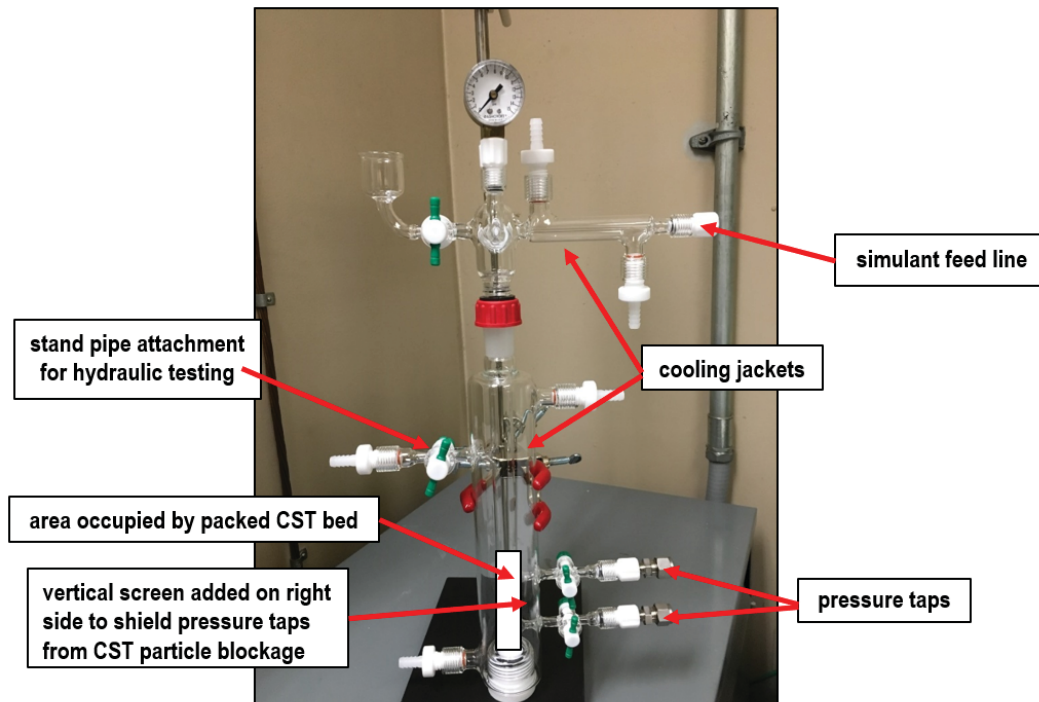


Figure 2-5. Ion Exchange Column Design.

instantaneous cesium breakthrough from the column rather than bucket average breakthrough. Although the CST masses were the same for each column, the packed bed volumes varied because the CST bed densities varied between batches (see Table 2-5). The height of the IE-911 CST bed, which had the highest bed density (1.0292 g dry CST/mL) was only 10.7 cm, while the height of the 9140-B CST which has the lowest bed density (0.9332 g dry CST/mL) was 11.7 cm, which is 16% higher than the height observed with IE-911. The presence of the side screens within the columns also effected the bed height. Based on the measured heights of the CST columns and the known (previously measured) CST bed densities, the apparent diameter of each column is provided in the table taking into account diameter constriction from the screens.

Simulant was pumped through the columns in a downflow direction. The liquid flow rate through the columns was checked at least daily by collecting 10 mL simulant effluent sub-samples over a known elapsed time. The pumps were adjusted as needed to achieve the target flowrate of 1.2 mL/min. The cumulative mass of effluent collected from each column was determined (ignoring sub-sample volumes which account for <1% of the total volume) and recorded on at least a daily basis and overall flow rates were calculated based on these masses. Note that the same target flow rate was used for each column, although the CST bed volumes were different. As a result, the flowrates on a BV/hr basis were not identical, as shown in Table 2-6. The cumulative average flow rates ranged from 3.1-3.4 BV/hr. During approximately the first half of processing with Column B, the flow rate was lower than the target. The flow was stopped and the pump was changed at this point and the flow rate with the new pump was closer to the target. As a result,

there was a small step change in flow rate for Column B and the overall flow rate was slightly below the target value and the %RSD for the average flow rate was higher, as indicated in Table 2-6. Flow rate data for each column in BV/hr units is provided graphically in Figure 2-6. The BVs of solution processed at each sub-sampling event were assigned based on these flow rates.

Table 2-5. Masses, Bed Densities, and Dimensions for CST Columns.

Column ID	CST Media	Hydrated CST (g)	Dry CST (g)	Dry Bed Density (g/mL) ^a	Bed Height (cm)	Apparent Column Diameter (cm) ^d	Packed Bed Volume (BV in mL)
A	IE-911	25.9564	21.7714	1.0292	10.1	1.63	21.2
B	9120-B ^c	26.8870	21.8992	0.9711	10.8	1.63	22.6
C	9140-B	25.9891	21.7898	0.9332	11.7	1.59	23.3

^a measured in graduated cylinders prior to testing

^b apparent diameter is smaller than the glassware ID due to presence of screens along one side of the beds

^c Lot #2099000035

^d actual column ID: 1.75 cm

Table 2-6. Simulant Volumes Processed and Flow Rates for CST Column Tests.

Column ID	CST Media	Processing Range (BV)	Average mL/min	Average BV/hr	BV/hr %RSD	Total Liquid Processed (L)
A	IE-911	0-1882 (cumulative)	1.20	3.39	3.7	39.8
B	9120-B ^a	0-963	1.08	2.88	5.1	21.6
		963-1796	1.23	3.26	5.1	18.3
		0-1796 (cumulative)	1.15	3.06	8.5	39.9
C	9140-B	0-1708 (cumulative)	1.19	3.07	4.4	39.9

^a Lot #2099000035

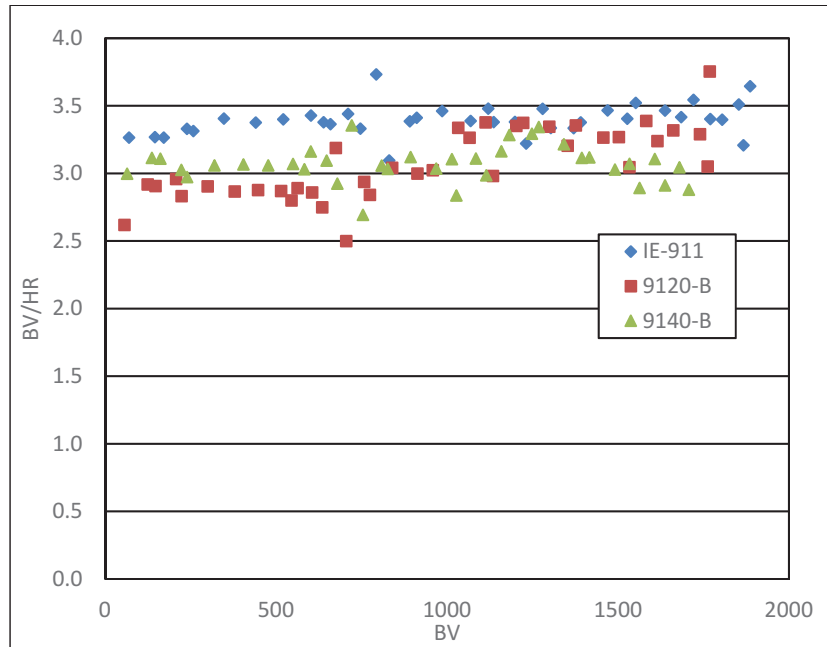


Figure 2-6. Flow Rate Data for Each Column.

2.7 ZAM Isotherm and VERSE Column Model Calculations

The ZAM Isotherm Model code is purchased commercial software developed at Texas A&M University by Z. Zheng, R. G. Anthony, and J. E. Miller designed to simulate ion-exchange equilibria of electrolytic solutions and CST solids. The ZAM code is a product of several years of development and research in Professor R. G. Anthony's Kinetics, Catalysis and Reaction Engineering Laboratory in the Department of Chemical Engineering Texas A&M University. A description of the current ZAM model is available [14].

The ion exchange media is an engineered form of crystalline silicotitanate that is composed of submicron-sized CST “powder” bound into a bead with a binding agent. The ZAM model only calculates the CST media performance in its powdered form. Therefore, to adjust for the engineered CST media, a fixed amount of engineered-form media must be mathematically converted into its powdered form (i.e., to maintain the actual amount of exchange sites present in each batch contact sample) by multiplying the CST dry mass by a binder mass dilution factor (DF). Once the media is put into its equivalent powdered-form dry mass basis, ZAM calculations are performed. Upon completion of the ZAM batch contact calculations, the resulting cesium loadings and distribution coefficient (K_d) values are then converted back to an engineered-form basis. All ZAM calculations were made using software version-4. Although version-5 was developed to improve the calculated competition between SrOH^+ and Cs^+ , the outcome is identical to version-4 in SRS tank waste compositions and version-4 converges better than the later version-5. Beta (β) factors calculated for SRS Average Simulant at various temperatures and an equation describing the temperature dependence are provided in Appendix B.

The VERSE-LC column model code was employed to perform CST column predictions to estimate Cs breakthrough performance for the TCCR project. VERSE has been SRNL's tool of choice for this since 2002 [7].

2.8 Column Hydraulic Testing

Following the conclusion of cesium performance testing, the ion exchange columns were stored with the CST beds immersed in SRS Average Simulant under ambient conditions for several weeks prior to starting hydraulic testing. The tests were conducted on each column by attaching a glass manometer to the pressure taps on the sides of the columns. These pressure taps were separated by 2 inches in height and spanned the central portion of the packed CST bed. The upper pressure tap was at least 1 cm below the top of the packed bed and the lower tap was at least 1 cm above the bottom of the bed. This configuration was intended to eliminate end packing effects on the bed porosity and pressure drop measurements. A photograph of the manometer is provided in Figure 2-7. The manometer was prepared from ~1 cm ID glass tubing and the manometer tubes were ~30 inches tall. The tops of the two manometer tubes were open to the atmosphere. The plastic tubing extending horizontally toward the left from the bottom of the manometer tubes was attached to the pressure taps on the columns using Swagelok™ fittings. A ruler was positioned between the manometer tubes to measure the liquid heights in the tubes. Minimal air bubbles were present in the horizontal tube portions such that a solid column of liquid connected the manometer tubes and the column. Transferring additional simulant into the columns with the bottom column valve closed and the top vented resulted in the formation of a liquid head above the CST bed. Opening the stopcocks on the pressure taps subsequently resulted in the flow of simulant into the manometer tubes. The tubes filled to the same liquid height as the liquid within the column head. Under stagnant conditions (no flow through the columns) there was no difference between the liquid heights in the two manometer legs, indicating that static pressure differences between the pressure taps were cancelled out with this manometer design. At the higher flow rates tested, the height of the column was insufficient to contain the liquid head and it was necessary to attach a stand pipe to the column to achieve an adequate liquid height. A glass standpipe with a 1 cm ID was attached to the column at the location indicated in Figure 2-5 and the vent was closed on the top of the column. The column and the manometer were adjusted to vertical positions using a level prior to conducting hydraulic testing. Prior to testing, the column temperature was adjusted to 24 °C using the water recirculating unit. The recirculating unit stopped working during hydraulic testing of Column B and the column temperature increased slightly during testing due to heating of the simulant by the pump. As a result, the relative standard deviation of the temperature data for this test was larger.

Upon the initiation of simulant flow through the columns (after opening the bottom stopcock), a liquid height increase was observed in the column head above the CST and a height difference was observed to form between the liquid levels in the manometer tubes over the course of several minutes. The height difference between the liquid in the manometer tubes under these dynamic flow conditions corresponds to the frictional pressure drop across the 2-inch section of the bed. As measured and recorded the units of height difference were cm of simulant per 2 inches of bed. The pressure drop data was converted to inches of water per inch of CST units using the densities of water and simulant. Liquid was recycled through the columns during hydraulic testing using a 1 L bottle of simulant.

An initial simulant flow rate of 2-3 mL/min was used to determine the frictional pressure drop across the packed CST bed. After stabilization of the liquid levels in the column and the

manometer (typically required 15-30 minutes), the manometer and column liquid heights were recorded. The flow rate was measured by collecting simulant from the column over the course of 1 minute and measuring the simulant mass. The simulant masses were converted to volume using the known density. The flow rate through the column was subsequently increased stepwise and the process was repeated. The maximum flow rates tested for the columns ranged from 17-32 mL/min. A flow rate of 32 mL/min corresponds to a superficial velocity near 14 cm/min. The flow rate of 5 gpm used during much of the TCCR Batch 1A processing corresponds to a superficial velocity of ~10 cm/min. The flow rate used for cesium performance testing with these columns was near 1.2 mL/min. Therefore, the flowrates evaluated during hydraulic testing covered the range of flowrates used in both the laboratory and field conditions. After the maximum flow was evaluated, the flowrate was decreased stepwise across the same range used during periods of increasing flowrate. In general, no hysteresis effects were observed, and similar pressure drop values were collected during periods of decreasing flow rate as were observed during periods of increasing flow rate. Longer stabilization periods were typically used immediately after changing from increasing to decreasing flow rates, since this point in the experiment involved some meniscus inversion within the manometer. In addition, two full hydraulic cycles with ascending and descending flow rates in each cycle were conducted for one column and consistent results were observed between the cycles.



Figure 2-7. Glass Manometer Used for Column Hydraulic Testing.

2.9 CST Particle Size Determination

To evaluate the column hydraulic results, the average particle diameter of each CST batch was determined based on vendor-provided sieve data. This analysis was reported previously for the IE-911 CST [1]. The vendor sieve data for the 9120-B (Lot 2099000035) and the 9140-B CST batches are provided in Tables 2-7 and 2-8, respectively. Computation of an average spherically equivalent particle diameter for the CST beads required generation of a cumulative distribution function based on a log-normal fit for weight percent passing versus sieve size. Once the cumulative distribution function was determined for each test sample, probability distribution functions on a weight and number basis were computed. The calculated cumulative distribution functions for the two CST batches are provided in Figures 2-8 and 2-9. Given the probability distribution function of the particle distribution on a number basis, the volume-based mean spherically equivalent diameter was computed based on the definition provided in The Powder Technology Handbook [15].

For report revision 2, Microtrac particle size analysis of sub-samples of the actual column test samples was conducted (see Section 3.7).

Table 2-7. 9120-B Lot 2099000035 CST Vendor Sieve Data.

Screen Cut (mesh)	Size Range (μm)	Weight Percent (%)
+18	<1000	0.1
18-20	1000-841	6.4
20-25	841-707	16.0
25-30	707-595	17.2
30-35	595-500	30.3
35-40	500-420	20.3
40-50	400-297	9.4
-50	<297	0.5

Table 2-8. 9140-B Lot 2002009604 CST Vendor Sieve Data.

Screen Cut (mesh)	Size Range (μm)	Weight Percent (%)
+18	<1000	0.6
18-20	1000-841	9.5
20-25	841-707	16.9
25-30	707-595	24.3
30-35	595-500	28.6
35-40	500-420	11.1
40-50	400-297	8.6
-50	<297	0.2

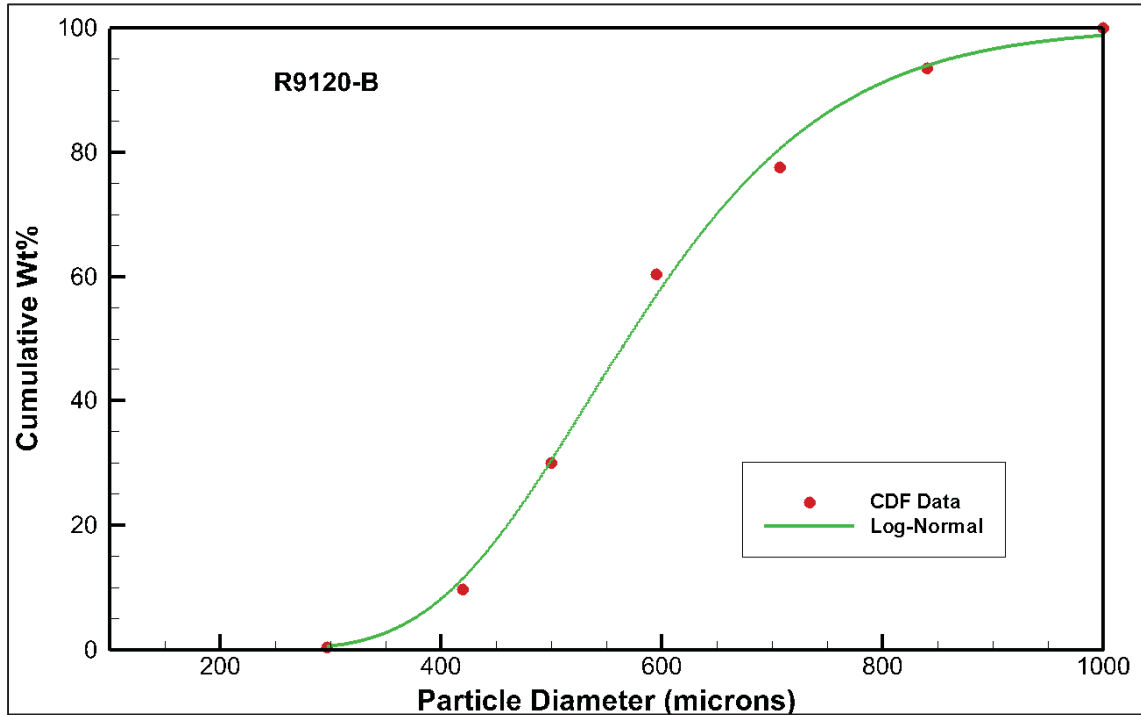


Figure 2-8. Cumulative Particle Diameter Distribution Function for CST Batch 9120-B Lot 2099000035 Based on the Vendor Sieve Data in Table 2-7.

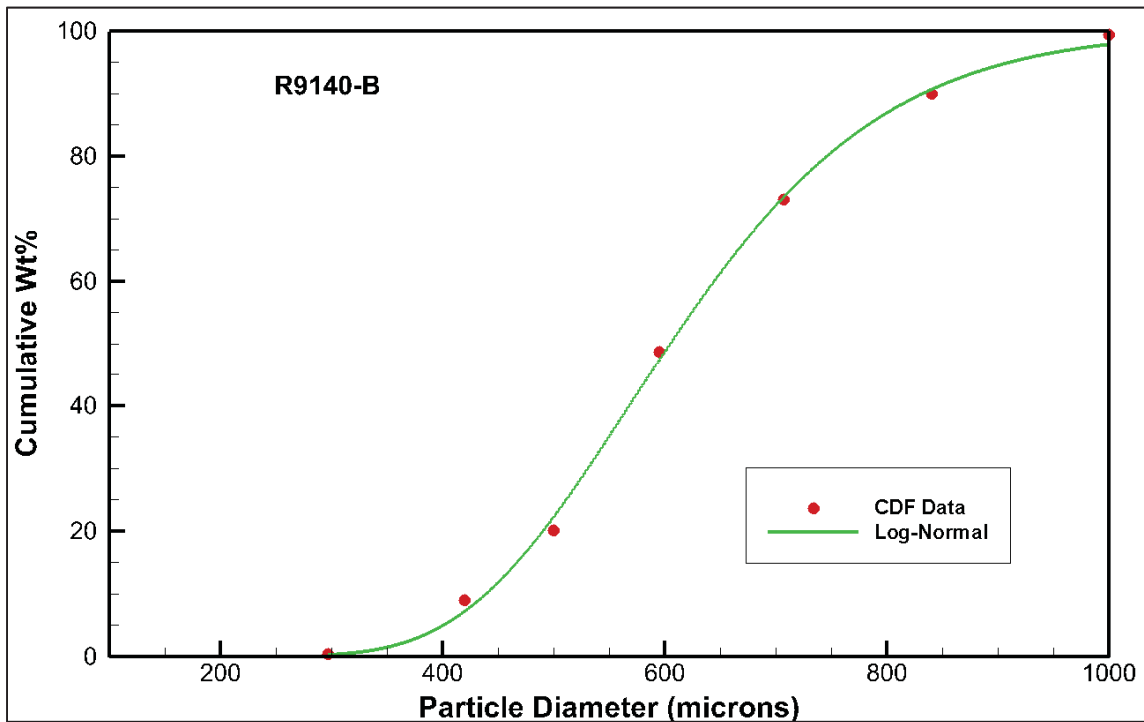


Figure 2-9. Cumulative Particle Diameter Distribution Function for CST Batch 9140-B Lot 2002009604 Based on the Vendor Sieve Data in Table 2-8.

3.0 Results and Discussion

3.1 CST Batch Contact Equilibrium Test Results

Based on the ICP-MS results, cesium distribution coefficients (K_d ; Equation 1), % removal (Equation 2), and loading (mmol Cs^+ /g CST; Equation 3) values were calculated for each batch contact test sample.

$$K_d = \left[\left(\frac{C_i}{C_f} \right) - 1 \right] \left[\frac{V}{MF} \right] \quad (\text{Equation 1})$$

$$\% Cs^+ \text{ Removal} = [(C_i - C_f)/C_i][100] \quad (\text{Equation 2})$$

$$Q = (C_i - C_f)(V)/(MF) \quad (\text{Equation 3})$$

where,

- K_d - distribution coefficient, (mL/g) on a dry mass basis
- C_i - initial liquid-phase Cs^+ concentration, [M]
- C_f - final (i.e., equilibrium) liquid-phase Cs^+ concentration, [M]
- V - liquid-phase volume, (mL)
- M - CST in hydrated reference state mass, (g)
- F - mass correction factor for CST water content, and
- Q - total Cs^+ loading.

Simulant batch contact equilibrium cesium loading results for the three CST batches are provided in Table 3-1. Cesium loading results were consistent between replicate samples as indicated by the low %RSD values. Cesium distribution coefficients (K_d 's) at 35 °C (near the TCCR operational temperature) ranged from near 900 mL/g (~90% Cs^+ removal) for batches 9120-B and 9140-B to near 1100 mL/g (~92% Cs^+ removal) for the archived IE-911 batch at an average liquid-to-solid phase ratio of 97 mL/g dry CST. These results indicate that the IE-911 batch has a higher cesium capacity than recently prepared batches. The results also indicate that the minor TCCR CST 9120-B media lot (2099000035) has similar cesium removal performance to the major TCCR lot (2099000034). Batch contact equilibrium tests were also conducted at 25 °C for the IE-911 CST batch to evaluate whether the cesium distribution coefficient with this simulant batch was similar to previous results [1] where the cesium K_d was near 2,300 mL/g (slightly lower temperature of 23 °C and higher phase ratio of 115 mL/g in previous tests). The measured K_d of 1,432 mL/g at 25 °C for the recently prepared SRS Average simulant was lower than previous results. Based on this result, it appears that some component in the simulant solution used for these equilibrium studies may have resulted in reduced cesium loading on the CST media (see additional discussion in Sections 3.3 and 3.7).

3.2 ZAM Isotherm Modeling of the Batch Contact Data

The calculated ZAM model dilution factors (DF) are also provided in Table 3-1. A plot of the ZAM-predicted cesium equilibrium loading isotherm for SRS Average Simulant at 35 °C with the experimental batch contact data included is provided in Figure 3-1. A binder dilution factor (DF)

Table 3-1. Cesium Equilibrium Distribution Coefficients (K_d), % Removal, Loading and Calculated ZAM DFs for Various CST Batches with the SRS Average Simulant Batch Used for Column Testing.

CST Batch/Sample ^a	Temperature (°C)	Cs ⁺ K_d (mL/g) ^b	Cs ⁺ % Removal	mmol Cs ⁺ /g CST ^b	ZAM Dilution Factor (DF)
Archived VP IE-911	25 ^c	1425	93.7	4.1E-03	0.614
		1440	94.3	3.7E-03	0.619
	35	1121	92.2	3.8E-03	0.625
		1061	91.7	3.9E-03	0.592
		989	91.5	3.7E-03	0.552
FP 9120-B (Lot 2099000034)	35	924	90.3	3.9E-03	0.517
		890	90.0	3.9E-03	0.498
FP 9120-B (Lot 2099000035)	35	923	90.1	4.0E-03	0.516
		860	89.5	3.9E-03	0.482
VP 9140-B	35	885	90.1	3.8E-03	0.495
		862	89.8	3.8E-03	0.482

^a FP = field-pretreated, VP = vendor pretreated

^b dry engineered CST mass basis

^c Note: An oven thermocouple error discovered at test completion did not allow confirmation that the temperature throughout testing was at the target value.

is typically utilized for engineered CST to account for mass contributions from the binder material. In cases where CST performance is lower than expected, this factor includes corrections for the binder and for low performance. A DF of 0.5 was required for the 9120-B and 9140-B batches to bring calculations into agreement with measurements while a DF near 0.6 (20% higher) was required for the IE-911 batch at 35 °C. These dilution factors are lower than recently observed with a different SRS Average Simulant batch [1, 2]. A DF of 0.68 has typically been used for engineered CST batches [7], but a DF of 1.0 was reported for IE-911. This indicates a 26% cesium capacity reduction for the 9140-B CST and a 40% reduction for the IE-911 CST relative to previous test results with the same CST media, but a different simulant batch. Since analysis results for the simulant batch utilized for testing were as expected with no indication of impurities and the simulant was filtered twice prior to testing, the reason for the low performance was not understood prior to the post-test additional analysis discussed in Section 3.7

3.3 CST Column Results

Column tests were also conducted with each CST batch and SRS simulant at 35 °C using 21.8 g samples of dry CST (based on mass corrections for water content) packed within each of three 1.6 cm ID jacketed glass columns. The SRS Average Simulant was pumped through the columns at an average flow rate near 1.2 mL/min (3.0-3.4 CST column bed volumes of simulant per hour). During the first few hours of column testing, a brown residue was observed to form on the top portions of each CST column (column photographs provided in Figures 3-2 through 3-4). Small (~3 mL) sub-samples of the column effluents were collected periodically to determine the instantaneous cesium breakthrough profiles. Breakthrough profiles plotted on a CST BV basis

(1 BV = volume of solution processed through column equal to packed media bed volume) for each CST batch are provided in Figure 3-5. Nearly linear cesium breakthrough profiles were observed for each column under these conditions. The maximum cesium breakthrough concentrations ranged from 81% (IE-911) to 92% (9140-B) of the feed concentration after processing approximately 40 L of simulant through each column. Significantly greater bed volumes of simulant were processed with the IE-911 CST prior to reaching the 50% cesium breakthrough point relative to the other two CST batches. The 50% cesium breakthrough points were observed near 800 BV for the 9120-B and 9140-B CST and near 1120 BV (40% higher than the other batches) for IE-911.

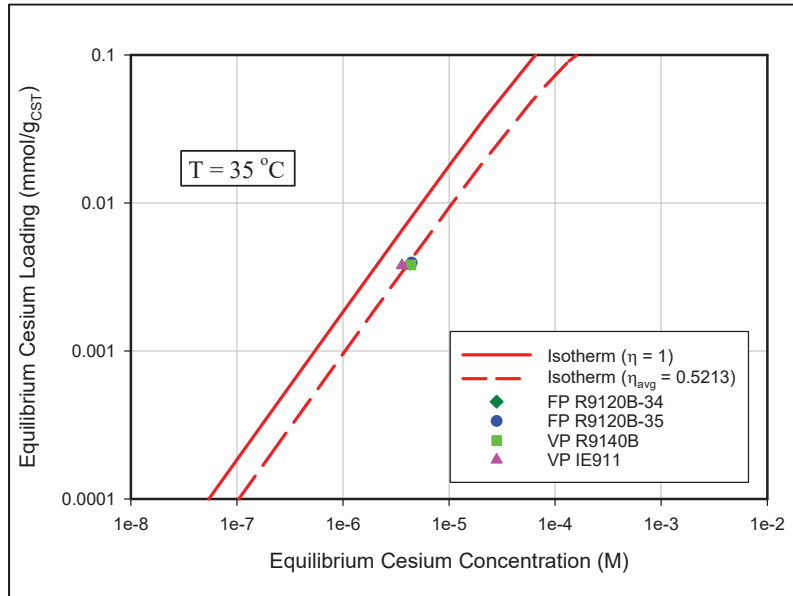


Figure 3-1. ZAM Isotherm Predictions Versus Observed Batch Contact Data.



Figure 3-2. Brown Residue Observed on the Top of the IE-911 CST Column During Testing.



Figure 3-3. Brown Residue Observed on the Top of the 9120-B CST Column During Testing.



Figure 3-4. Brown Residue Observed on the Top of the 9140-B CST Column During Testing.

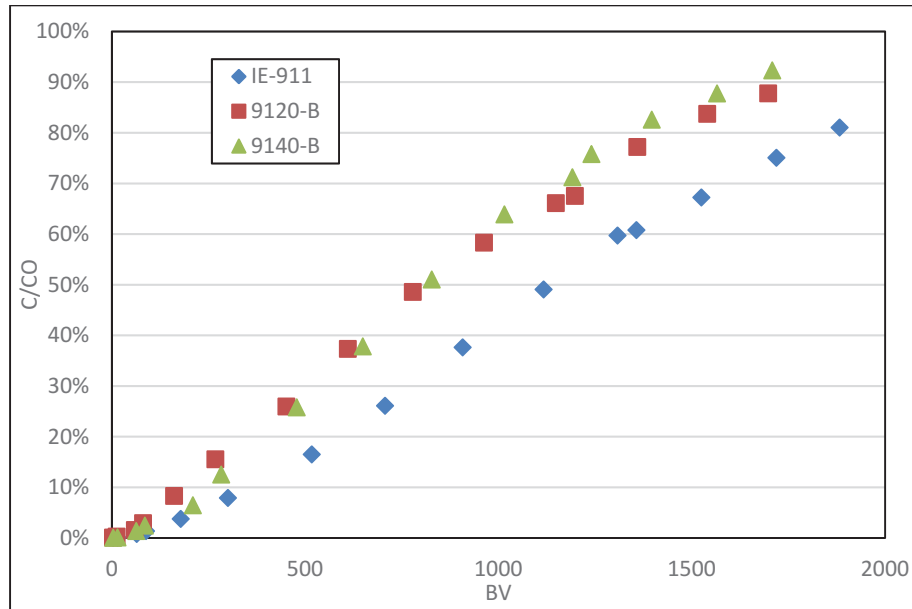


Figure 3-5. Cesium Column Instantaneous Breakthrough Profiles Versus Simulant BVs Processed for Three CST Media Batches at 35 °C at Flow Rates of 3.0-3.4 BV/hr.

Plotting these results on a bed volume basis incorporates bed density differences between the CST batches. The packed bed density of IE-911 CST (1.029 g dry CST/mL bed) is 10% higher than the density of 9140-B CST (0.9332 g dry CST/mL bed). Plotting the breakthrough data versus the cumulative simulant volume processed (Figure 3-6) reveals that with equal masses of CST in the columns the 50% breakthrough points occurred after processing 18-19 L of simulant for 9120-B and 9140-B CST and after processing 24 L of simulant (30% higher than observed with the newer CST batches) for IE-911. Later cesium column breakthrough is consistent with trends in the batch contact data and indicates that the IE-911 CST has higher cesium capacity than the other CST batches. Higher bed density results in further performance improvement of IE-911 relative to the other batches, since for a given column volume a greater mass of CST can be added. The combined effects of higher capacity and higher density for IE-911 CST resulted in 40% more column bed volumes processed to reach 50% cesium breakthrough, as discussed in the previous paragraph.

The early portions of the column cesium breakthrough profiles are provided in Figure 3-7. The cesium concentrations for all three profiles increased dramatically and approached or exceeded 1% Cs⁺ breakthrough after processing 60-90 BV of simulant. The breakthrough profiles reached a decontamination factor of 1000 (0.1% breakthrough) after processing 15-60 BV of simulant. For the IE-911 column, 0.05% and 0.8% Cs⁺ breakthrough were observed after processing 15 and 67 BV of simulant, respectively. For the 9120-B column 0.05% and 0.25% Cs⁺ breakthrough were observed after processing 13 and 60 BV of simulant, respectively. For the 9140-B column 0.09% and 1.4% Cs⁺ breakthrough were observed after processing 15 and 65 BV of simulant, respectively. The average particle diameter of IE-911 CST is smaller than that of the recently prepared batches (volume-based mean particle diameter: 408 μm for IE-911, 583 μm for 9120-B, and 614 μm for 9140-B). Cesium breakthrough for all three columns was more rapid than expected. The detectable limit of the instrument for cesium in this solution was 0.02% of the feed concentration.

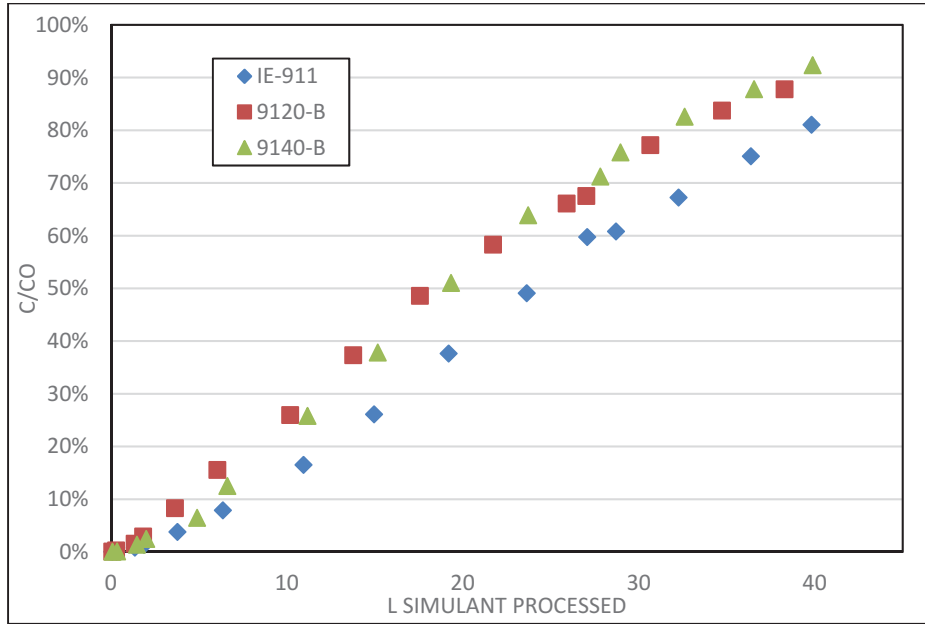


Figure 3-6. Cesium Column Instantaneous Breakthrough Profiles Versus Cumulative Simulant Volume for Three CST Media Batches at 35 °C at Flow Rates of 3.0-3.4 BV/hr.

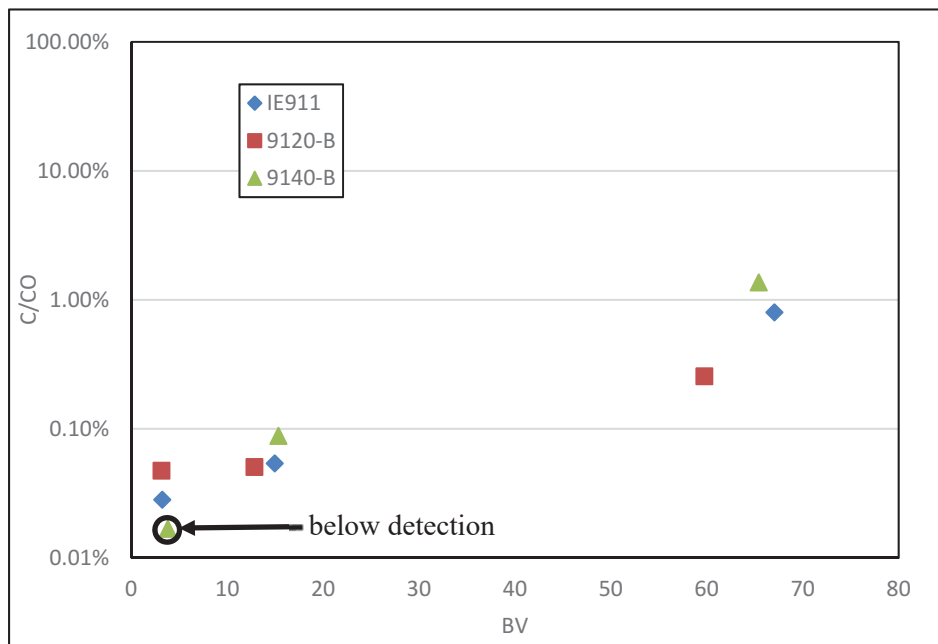


Figure 3-7. Initial Cesium Column Instantaneous Breakthrough Profiles for Three CST Media Batches at 35 °C at Flow Rates of 3.0-3.4 BV/hr.

The cesium removal performance results are consistent with fouling of the CST media. As shown in Figures 3-2 through 3-4, a brown residue was observed to form on the top portions of each CST column during the first few hours of column testing. It is possible that fouling may have occurred, and this may explain the reduced cesium capacity and performance of the CST batches during column testing. Analytical results for the simulant batch utilized for testing were as expected with no indication of impurities (Table 2-2). Despite the indication of media fouling, it is apparent from the data that the IE-911 CST media is superior in performance to the recently-prepared CST batches with regard to cesium loading capacity and density such that significantly greater volumes of waste could be processed for a given column volume. This finding is consistent with earlier testing on these CST batches [1, 2].

3.4 VERSE Column Modeling

The VERSE model predictions of the cesium column breakthrough profiles for the IE-911 and 9140-B CST columns at 35 °C utilizing the DF values derived from the batch contact testing (Table 3-1) and a tortuosity factor (τ) of 4.0 are provided in Figure 3-8 and compared to the experimental data. At 35 °C, the 50% breakthrough points were predicted to occur at approximately 669 and 929 BV, respectively, for 9140-B and IE-911. The experimental 50% breakthrough points were later than predicted indicating that better cesium removal performance was observed in the column tests than in the most recent batch contact equilibrium tests with this simulant batch. The experimental cesium breakthrough profiles are also much less sharp than predicted indicating slower cesium loading kinetics than expected. A semi-log plot of the data is provided in Figure 3-9 to emphasize the differences between the early experimental data and predictions.

Adjustments to the VERSE parameters were subsequently made (Figure 3-10) such that the model predictions would match the experimental data. The dilution factor is typically used to reduce the amount of active exchange sites relative to powder CST and the tortuosity factor, τ , is used to reduce the cesium diffusivity in the CST media pores relative to the bulk solution diffusivity. A DF of 0.757 and τ of 10.0 were required to fit the experimental breakthrough profiles for IE-911. A DF of 0.616 and a τ of 6.0 were required to fit the experimental profile for 9140-B CST. A τ of 4.0 is typically used for CST media. The results indicate that the CST media performance for all the media samples tested with this simulant batch are significantly reduced relative to previous testing. Both batch contact and column data indicate reduced cesium capacity. The DF difference between the column and batch contact data are not understood. Column data would be expected to give more accurate cesium loading results than batch contact data. Lower DF values for the batch contact tests may be due to the achievement of less than 100% equilibrium in the batch contact tests (expected to exceed 90% of equilibrium based on previous testing) or some compositional change that may have occurred with the simulant during the interim period between batch contact and column testing. The column data also indicates reduced cesium loading kinetics relative to previous results with these materials and historical data. VERSE model predictions for these CST batches based on historical testing (blind prediction) are provided in Figure 3-11 where it is apparent that cesium breakthrough occurred earlier than expected. The observed 50% cesium breakthrough point of ~800 BV for the 9120-B CST was 16% lower than the predicted value of 929 BV based on a DF of 0.68. The 50% cesium breakthrough point for the IE-911 CST of 1120 BV was 29% lower than the predicted value of 1574 BV based on a DF of 1.0. It should be emphasized that a DF of 1.0 implies that no binder mass correction is needed for engineered CST, which does not make physical sense unless the binder contains comparable and identical ion exchange sites to the powder form of CST. If no correction factor (DF = 1.0) is needed for IE-

911, this likely means that the CST ion exchange capacity in the ZAM model is incorrect for this media batch.

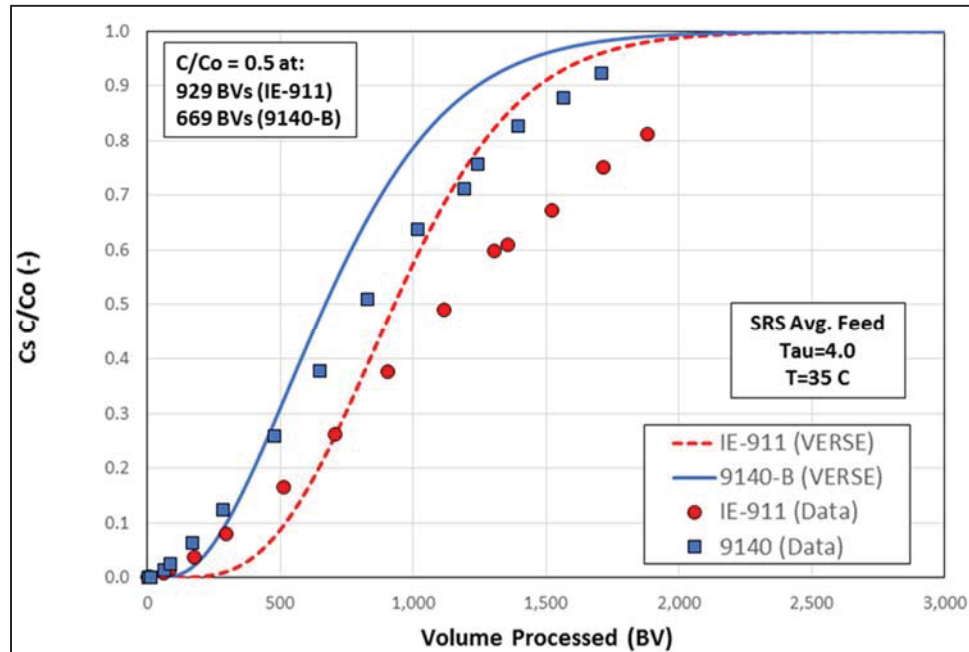


Figure 3-8. VERSE Model Predictions Versus Instantaneous Measured Cesium Breakthrough Profiles for IE-911 (DF = 0.60) and 9140-B CST (DF = 0.50) at 35 °C at the Average Flow Rates Used for Testing of 3.0-3.4 BV/hr (DFs based on Table ES-1 K_d data collected using the simulant batch utilized for column testing).

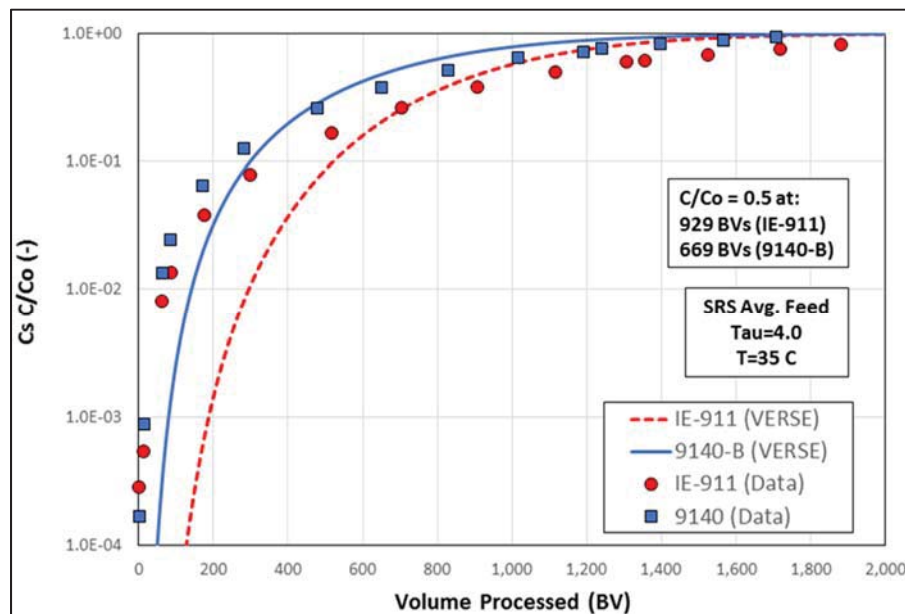


Figure 3-9. Semi-log Plot of VERSE Model Predictions Versus Instantaneous Measured Cesium Breakthrough Profiles for IE-911 (DF = 0.60) and 9140-B CST (DF = 0.50) at 35 °C at the Average Flow Rates Used for Testing of 3.0-3.4 BV/hr (DFs based on Table ES-1 K_d data collected using the simulant batch utilized for column testing).

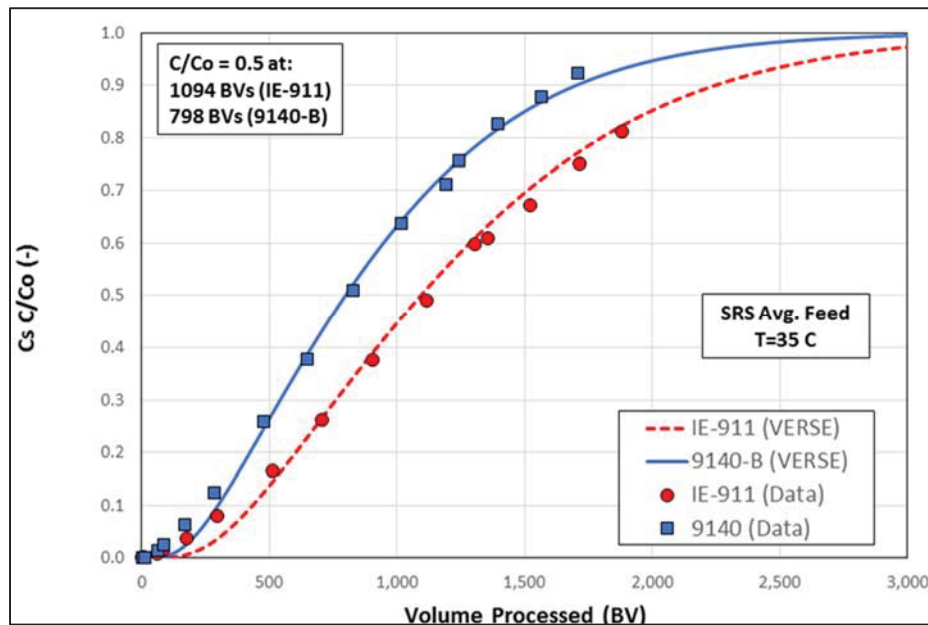


Figure 3-10. VERSE Model Predictions Versus Measured Cesium Instantaneous Breakthrough Profiles for IE-911 (DF = 0.757 and $\tau = 10.0$) and 9140-B CST (DF = 0.616 and $\tau = 6.0$) at 35 °C at the Average Flow Rates Used for Testing (DFs and τ adjusted to fit column data).

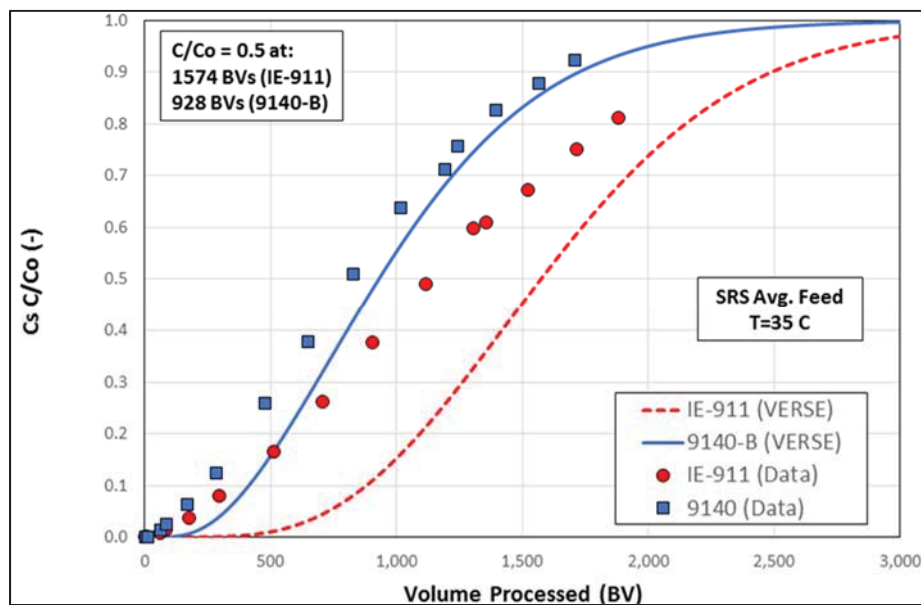


Figure 3-11. VERSE Model Predictions Versus Measured Cesium Instantaneous Breakthrough Profiles for IE-911 (DF = 1.0 and $\tau = 4.0$) and 9140-B CST (DF = 0.68 and $\tau = 4.0$) at 35 °C at the Average Flow Rates Used for Testing (expected performance based on historical testing).

3.5 Column Hydraulic Testing

After the completion of column testing for cesium removal performance, hydraulic testing was conducted with each column at ~ 24 °C (temperature increased to as high as 29 °C for a small number of datapoints) using SRS Average Simulant. As shown in Figure 3-12 and Table 3-2, the frictional pressure drop data was linear for each column across the full range of simulant flow rates evaluated. The linear regression analyses of the pressure drop data for each CST column were constrained to intercept the y-axis at zero and the R^2 values exceeded 99% in each case. The IE-911 column was evaluated at the highest flow rate (up to 13.5 cm/min). The frictional pressure drop data collected during test periods of decreasing flow rate followed the same trends as was observed during periods of increasing flow rate (i.e., no hysteresis effects). Across the range of flow rates evaluated, the highest pressure drop values were observed for the IE-911 CST column and the lowest were observed for the 9140-B CST column. Based on the data, IE-911 CST is expected to have 19% higher pressure drop than the TCCR 9120-B CST, while the 9140-B CST would be expected to have 28% lower pressure drop than 9120-B. Relative to IE-911 CST, 16 and 39% lower pressure drops, respectively, were observed for 9120-B and 9140-B CST samples. These percentages are based on the slopes of the linear regression analysis (0.10 for IE-911; 0.088 for 9120-B; 0.063 for 9140-B).

The order of increasing pressure drops is consistent with the order of decreasing average particle diameters calculated from sieve data provided by the vendor for each CST batch. The volume-based mean particle diameters were determined to be: 408 μm for IE-911, 583 μm for 9120-B, and 614 μm for 9140-B. However, given the similarities in the average particle diameters for the 9120-B and 9140-B CST batches, the pressure drop data for these two CST batches was expected to be closer than was observed. The vendor sieve data that the particle size analysis was based on was from the large-scale manufacturer batch, rather than the actual samples tested. Sub-sampling errors may explain this discrepancy. In addition, the pressure drop is primarily a function of the packed bed porosity (which is significantly influenced by the polydispersity in the CST particle diameter) and may not correlate exactly with the volume-based mean diameter.

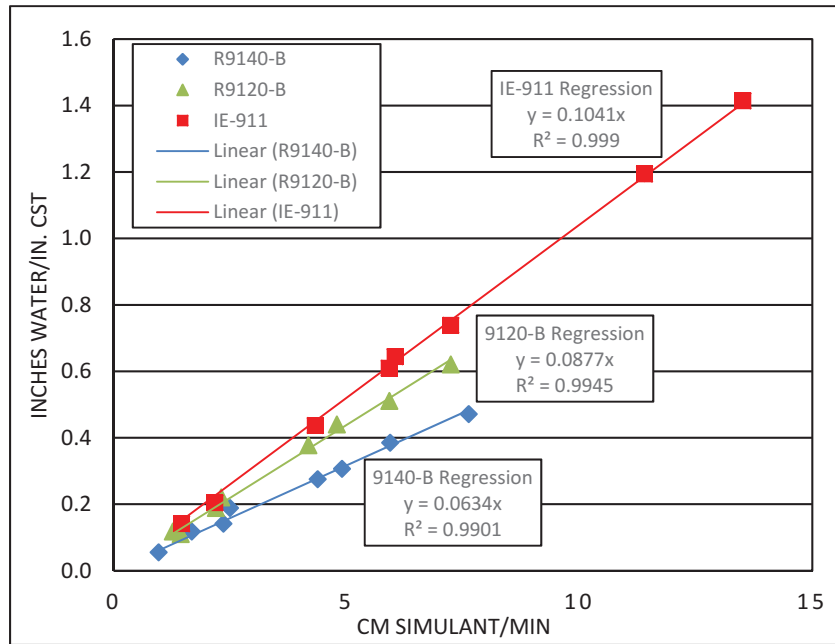


Figure 3-12. Frictional Pressure Drop versus Flow Rate Profiles for CST Columns Measured in SRS Average Simulant at 23-30 °C (only Cycle 2 data plotted for 9140-B).

Table 3-2. Frictional Pressure Drop Data for CST Columns.

CST Batch (Column)	T (°C)	mL/min	cm/min	in water/inch of CST
IE-911 (Col. A)	24.1	3.5	1.5	0.14
	24.5	5.2	2.2	0.20
	24.2	10.4	4.3	0.44
	24.2	14.2	5.9	0.61
	23.9	17.4	7.2	0.74
	24.0	27.4	11.4	1.19
	24.2	32.5	13.5	1.41
	24.0	14.5	6.0	0.64
	24.1	Average Temp.	---	
	0.8%	Temp. %RSD	---	
9120-B (Col. B)	23.8	3.0	1.3	0.12
	23.9	5.3	2.2	0.19
	23.9	10.1	4.2	0.38
	23.9	14.2	5.9	0.51
	23.8	17.4	7.2	0.62
	24.0	11.5	4.8	0.44
	29.0	5.5	2.3	0.22
	29.0	3.4	1.4	0.11
	25.2	Average Temp.	---	
	9.4%	Temp. %RSD	---	
9140-B (Col. C)	Cycle 1			
	---	2.9	1.2	0.06
	23.1	4.2	1.8	0.11
	23.6	6.9	2.9	0.18
	23.8	9.5	4.0	0.25
	23.6	13.3	5.5	0.34
	23.5	17.6	7.3	0.46
	23.8	15.1	6.3	0.38
	24.0	11.3	4.7	0.29
	23.6	Average Temp.	---	
1.2%	Temp. %RSD	---		
9140-B (Col. C)	Cycle 2			
	23.5	2.3	0.96	0.05
	23.8	5.7	2.4	0.14
	23.7	10.5	4.4	0.27
	23.6	14.3	5.9	0.38
	23.6	18.3	7.6	0.47
	23.8	11.8	4.9	0.31
	23.8	6.0	2.5	0.19
	23.8	4.0	1.7	0.12
	23.7	Average Temp.	---	
0.5%	Temp. %RSD	---		

Following the completion of hydraulic testing, the mobile (drainable) fluid fraction from separately packed beds of the three CST media samples used for testing was determined by measuring the drainable water (pH near 12) mass at ambient temperature using a 1-inch ID column. The mobile fluid volume fractions calculated based on the measured fluid densities were IE-911 – 18.0%; 9120-B – 22.9%, and 9140-B – 27.4%. This data is representative of the packed bed porosity and appears to correlate better to the trends in the hydraulic data than the mean particle diameter values based on sieve data.

3.6 Teabag Batch Contact Testing

SRR requested higher phase ratio (liquid volume/CST mass) teabag testing than was used in previous testing [3]. Two 15-liter plastic carboys were each loaded with 14.250 kilograms (11.37 liters) of cesium spiked SRS Average simulant. The phase ratio in both cases exceeded 113,000 mL/g. The two carboys were labeled 1 (current holder design) and 2 (new, more open holder design). This was a controlled test to determine how well the CST loads cesium to near saturation using the current and new teabag holders. Teabag batch contacts were conducted under unstirred conditions for 10 days with a single teabag suspended within the simulant in each carboy. Following completion of the first test (A), the teabags were subsequently unloaded, reloaded with new CST media samples, and used for Test B which served as a duplicate. The simulant in the carboys was re-used, but not re-spiked with cesium during teabag testing. The simulant cesium concentration decreased from 5.67 to 5.63 mg/L during Test A, which was not considered enough to require the addition of more cesium. No CST fines were observed throughout the testing.

Teabag units were placed in the holders and the holders were placed in the stainless-steel slotted vials (Figure 2-3). The vials were suspended in the carboys of simulant using wire hooks attached to the lifting lugs on the vials. Both carboys were stagnant (unstirred) throughout the tests. The carboys were placed in secondary containment in an area of the lab that would not be disturbed. M&TE temperature probes were placed in each secondary containment against the carboy walls, and temperatures were recorded each workday. Teabags were immersed at the same time, and each test ended 10 days after initial immersion. No heat was applied in the tests. Room temperature remained at 20 ± 1 °C for both Tests A and B. At the end of the test, each stainless-steel vial was lifted out of its carboy, the holder was removed, and the teabag unit was removed from its holder. Each teabag unit was exposed to the following rinses: 1) soaking in 65 mL of 0.01 M NaOH for 1 to 4 hours (as specified by procedure [13]) with occasional swirling, and 2) soaking in 65 mL of DI water for about 2 minutes. Each unit was then disassembled and the hardware parts including the CST were air dried for at least one day. Direct weighing of the CST and screens in each case deviated by less than a milligram from the CST mass calculated by difference using the entire assembled teabag unit mass (out of about 2.3 grams total) and the component part masses.

Analysis results for the teabag rinse liquids and the digested CST samples are provided in Tables 3-3 through 3-5. The loadings that are shown were corrected for 18 wt% moisture content; cesium loadings in the table represent moisture-free CST. The amount of cesium in the rinse solution was small and was therefore not included in the Cs loading calculations. Comparison of CST loadings in 10-day stagnant testing shows a definite improvement in loading for the new open teabag unit holder open design. Additional analysis results for selected CST components and sorbed ions from the teabag CST samples are provided in Appendix C.

ZAM calculations predict both cesium and potassium loadings. Table 3-4 shows that even with the new open teabag holder, the cesium DFs are 0.29 and 0.26. The first test with the current design showed very low cesium loading. The CST loads cesium at lower than expected levels. This agrees with the findings of teabag CST loadings in Tank 10 [12,16]; however, is in contrast to the earlier “unstirred” teabag testing where the loadings were only 16% below the ZAM prediction [3]. One possible explanation for this difference is the higher phase ratio used in the current work where low concentration impurities in the simulant may have loaded onto the teabag CST in amounts significant enough to impact the Cs removal. High phase ratio would provide opportunity for more impurities to be available for adsorption. If one or more of the impurities competes with cesium adsorption, then high phase ratio tests would show reduced cesium uptake compared to lower phase ratio tests. Table C-4 of Appendix C shows data for calcium and iron from the current carboy tests as well as the loadings found from Tank 10 Batch 1A CST. Calcium and iron data were chosen here because their uptake is highest of the elements measured and can exceed the mass or molar uptake of cesium on the CST. The uptakes of iron, despite difficulties of measuring its low concentration in solution, are highly significant. Its competition with cesium has not been assessed yet.

The ZAM DF for potassium, in contrast to cesium, compares well to the data. The type of holder (new versus current) barely makes a difference. The potassium DF is not far from unity for all four runs. To ascertain the source of the potassium, CST samples that were digested along with the carboy test samples were checked and showed less-than-detectable levels of potassium. Prior work also shows that potassium in as-received CST is below detection [10]. The potassium in this work was thus adsorbed from the simulant solution, showing that hydraulic contact of solution with the CST in the teabag was effective for potassium transport. Since potassium is at higher concentration than cesium in the liquid phase, and has less affinity for CST than does cesium, mass transfer needs may be less for the CST to reach its potassium equilibrium loading.

Table 3-3. Teabag Rinse Liquid Analysis.

Test	Carboy	Holder Design	Solution	Cesium (µg/L)	Total Cesium (µg)
A	1	Current	0.01 M NaOH	61.5	4
			DI Water	0.818	0.05
	2	New Open	0.01 M NaOH	104	6.76
			DI Water	2.04	0.13
B	1	Current	0.01 M NaOH	54.4	3.54
			DI Water	1.18	0.08
	2	New Open	0.01 M NaOH	67.9	4.41
			DI Water	0.91	0.06

Table 3-4. CST Cesium Loading and Liquid Cesium Concentrations

Test	Carboy	Holder Design	Final Liquid Cs ⁺ (M)	Cs ⁺ Loading (mmol/g) ^a	ZAM DF ^a
A	1	Current	4.27E-05	4.91E-03 ^b	0.065 ^b
	2	New Open	4.27E-05	2.28E-02	0.29
B	1	Current	4.23E-05	1.68E-02	0.21
	2	New Open	4.23E-05	2.02E-02	0.26

^a dry, engineered CST mass basis

^b the lower loading and DF for this sample versus the Test B replicate are not understood

Table 3-5. CST Potassium Loading and Liquid Potassium Concentration

Test	Carboy	Holder Design	Final Liquid K ⁺ (M)	K ⁺ Loading (mmol/g) ^a	ZAM DF for Potassium ^a
A	1	Current	1.50E-02	9.53E-02	1.09
	2	New Open	1.50E-02	1.11E-01	1.27
B	1	Current	1.50E-02	8.29E-02	0.95
	2	New Open	1.50E-02	8.41E-02	0.96

^a dry, engineered CST mass basis

3.7 Additional Characterization Data Following Test Completion

Following the completion of hydraulic testing, the columns were stored filled with simulant at ambient temperature for several months prior to being disassembled for removal and characterization of the CST media and the brown solids observed on the media. After test completion, a film of brown solids was also observed on the bottom of the simulant feed drum that had not been present prior to testing. These solids were also isolated and analyzed. Sub-samples of the simulant feed solution and effluent composite solution from each column were also analyzed in an effort to identify any potential contaminants that might have impacted the cesium removal performance. Finally, some additional analysis was conducted on CST standard blank samples for comparison to the test column CST digestion data.

Analysis results for the simulant feed sample indicated the expected bulk composition, confirmed that certain problematic species were not present above detectable levels, and identified other minor species that were present at low levels (Table 3-6). Calcium and iron, which were previously observed to load onto CST media from tank waste supernates [16], were below detectable levels in the simulant feed solution. Low levels (<150 ppb) of strontium, barium, tin, tungsten, zirconium, rubidium and lead were present in the simulant feed sample. Molybdenum was added as part of the simulant recipe and the molar concentration (2E-04 M) was an order of magnitude higher than the cesium concentration (4E-05 M). Zinc was present in the simulant feed solution at a molar concentration similar to cesium.

Table 3-6. Additional Simulant Feed and Column Effluent Analysis.

Component	Feed	Effluent Composite		
		IE-911 Column	9120-B Column	9140-B Column
µg/L				
<u>ICP-ES</u>				
Al	8.4E+06	---	---	---
K	6.0E+05	---	---	---
Mo	1.9E+04	---	---	---
Na	1.3E+08	---	---	---
P	3.1E+05	---	---	---
S	5.4E+06	---	---	---
Ca	<7.2E+02	---	---	---
Mg	<6.8E+01	---	---	---
Fe	<1.1E+03	---	---	---
Mn	<2.3 E+02			
Zn	2.4 E+03	---	---	---
Zr	<5.7E+02	---	---	---
<u>ICP-MS</u>				
Rb	30	30	34	33
Sr	78	<10	<10	<10
Zr	30	5220	6690	6350
Nb	<10	1350	1320	2340
Mo	19400	20000	20200	20100
Sn	40	46	46	47
Cs	5590	2330	2840	2920
Ba	136	<10	<10	<10
Hf	<10	359	496	488
W	37	48	47	45
Pb	25	<10	<10	<10
Total L Processed	---	39.8	40.3	39.9

Comparison of the feed and column effluent compositions revealed that the following species were removed to some degree by the CST media: Sr, Cs, Ba, and Pb. (Note that the total simulant volume processed through each column is provided at the bottom of the table. The total volume given for the 9120-B CST column is larger than was previously reported (Table 2-6), because some additional simulant (0.40 L) was processed through this column at the end of the cesium performance testing, though no analysis was conducted during this period to determine the cesium breakthrough profile.) Cesium was partially removed from solution during column processing, while the other metals (Sr, Ba, and Pb) were below detectable levels in all of the column effluent solutions. The cesium concentration in the effluent composite from the IE-911 column contained

the lowest cesium concentration of the three effluent solutions, which is consistent with the cesium breakthrough profiles and calculated dilution factors for the CST media batches. Surprisingly, there was no indication of rubidium (an alkali metal) removal by CST. No significant concentration differences were observed between the feed and effluent solutions for rubidium, molybdenum, tungsten and tin (zinc not analyzed in effluent). Metals observed to leach into the effluent solutions during contact with the CST columns resulting in dramatic increases in solution concentrations included: zirconium, niobium, and hafnium. Zirconium, niobium, and titanium (not analyzed in effluent solutions) leaching was expected from the CST media. Hafnium is likely a CST contaminant associated with the zirconia binder material (both metals are in Group 4 of the Periodic Table).

The loaded CST media samples were successfully recovered from each column by disassembling the columns and using water to remove residual simulant from the columns and sluice the CST media into beakers. During this process, it was readily apparent that the brown solids observed in the top portions of the columns were primarily precipitates that could be removed and separated from the CST media. (Note: A typical to low amount of CST fines were observed during washing.) The upper portion of each CST bed was initially removed from the columns along with the bulk of the brown solids and most of the solids were separated from the CST beads by decantation. The remainder of the CST was then removed from the columns. Column B (9120-B) CST beads were removed in successive 1 cm segments starting from the top as shown in Figure 3-13. Brown solids were observed in the upper 6 cm of the bed with the highest concentration in the top two segments. After washing and decantation, slightly discolored CST samples were isolated from the upper portions of each column (Figure 3-14). Sub-samples of the upper portion of each CST bed were submitted for analysis. A sub-sample of the bottom portion of the 9120-B CST column was also submitted for analysis. The CST samples isolated for analysis were placed in a drying oven at 35 °C for several days and dried to a constant mass prior to analysis. The brown solids isolated from the CST beds and the simulant drum were transferred to polymer bottles and most, but not all, of the wash water was removed (Figure 3-15). All four solid samples differed slightly in color, though all were tan or brown, indicating that the solids may have formed by separate precipitation events. Approximately 1 g of damp solids was isolated from the drum. This amount represents ~0.002 wt % of the total solids used for simulant preparation (~50 kg). Approximately 0.5 g of damp solids was isolated from each column. These amounts represent ~2 wt % of the CST mass in each column (26 g reference state mass).

Four CST sub-samples (three from the tops of the CST beds and one from the bottom) were digested in acid and analyzed by ICP-ES and ICP-MS. Analysis results are provided in Table 3-7. Dominant species observed were Ti, Nb, Zr, and Na, which are all primary sodium-form CST components based on the known composition. Comparison of the results for the column sub-samples to the average results for numerous CST digestion standard blanks (Table 3-8) indicates that the Ti and Nb concentrations are typical. However, Zr is 19-22% lower for the column sub-samples when compared to the standards, with the exception of the bottom of the 9120-B column. These results indicate that zirconium leaching occurred from the upper portions of the packed CST beds, but no significant leaching occurred from the bottom portion after processing approximately 40 L of simulant through the columns. Presumably an equilibrium exists between the zirconium in the solid CST binder and the simulant solution, and the leached zirconium present in solutions from the upper portions of the columns minimizes zirconium leaching from the lower portions of the columns. Other species observed in the CST sub-samples included: Al, Be, Ca, Fe, K, Li, Mg, Mn, Sr, Cs, Ba, Pb, Hf, and Ta. Lower metal loadings were generally observed for the

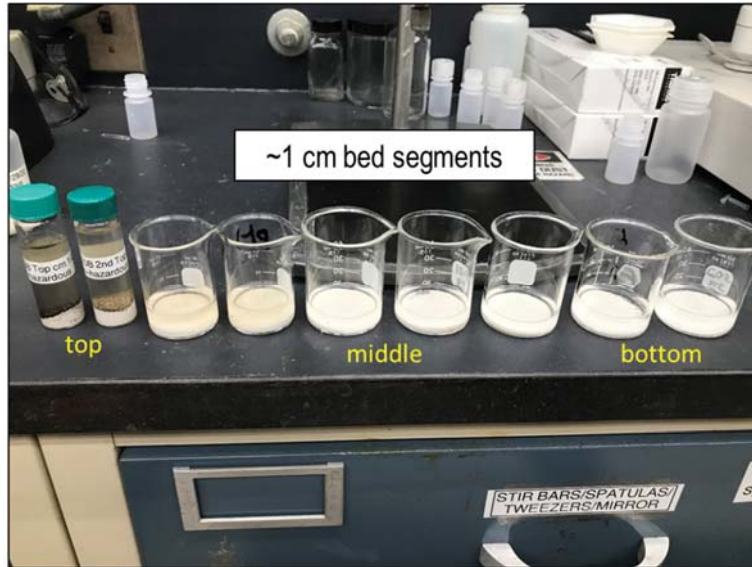


Figure 3-13. CST Samples Removed from 9120-B CST Column (Column B) in ~1 cm Segments.

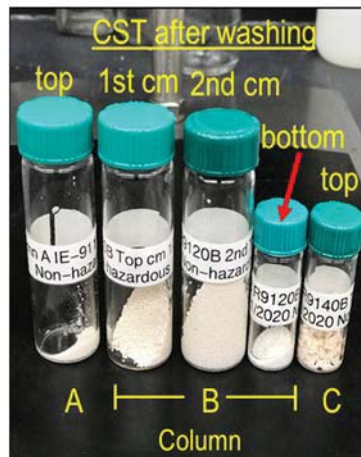


Figure 3-14. CST Samples from Upper Portion of Each Column (Column A = IE-911; Column B = 9120-B; Column C = 9140-B) and the 2nd and Bottom Portions of Column B after Isolation and Washing to Remove Precipitates.

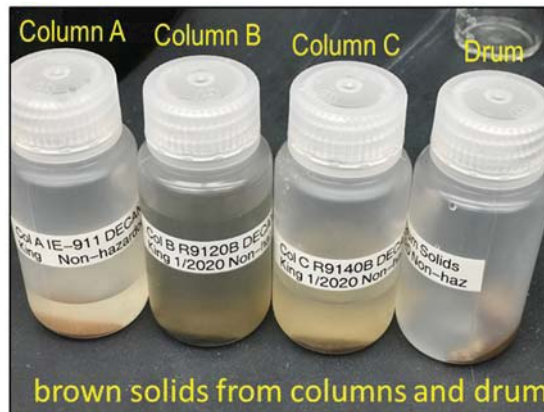


Figure 3-15. Brown Solids Isolated from the CST Columns and the Simulant Drum.

Table 3-7. ICP-ES and ICP-MS Data on Digested CST Column Sub-Samples After Cesium Performance and Hydraulic Test Completion.

Metal	IE-911 CST Bed <u>Top</u>	9120-B CST Bed <u>Top</u>	9120-B CST Bed <u>Bottom</u>	9140-B CST Bed <u>Top</u>
	µg/g reference state CST			
<u>ICP-ES Data</u>				
Al	2830	3160	3490	3220
Be	21	24	24	25
Ca	2340	5460	811	6030
Fe	1010	1110	761	996
K	2730	2450	2600	2600
Li	76	49	77	60
Mg	124	193	221	178
Mn	58	87	8	89
Na	6.46E+04	8.54E+04	8.45E+04	8.24E+04
Ti	1.57E+05	1.60E+05	1.58E+05	1.57E+05
Zr	8.67E+04	8.62E+04	9.92E+04	8.32E+04
<u>ICP-MS Data</u>				
Rb	<4.9	<2.7	<2.3	<1.8
Sr	181	379	<14	316
Zr	8.75E+04	8.24E+04	1.02E+05	8.15E+04
Nb	1.19E+05	1.25E+05	1.26E+05	1.28E+05
Cs	6100	5300	3990	7290
Ba	365	766	<9.4	727
Pb	17	15	5	11
Hf	1520	1430	1800	1440
Ta	267	165	162	178

Table 3-8. TCCR CST Digestion Standards Average ICP-MS and ICP-ES Data.

Metal	IE-911 CST	9120-B CST	9140-B CST
	μg/g reference state CST (%RSD)		
Ti	1.55E+05 (3.2)	1.55E+05 (3.4)	1.60E+05 (2.9)
Zr	1.09E+05 (1.6)	1.02E+05 (3.5)	1.04E+05 (1.8)
Nb	1.18E+05 (1.7)	1.21E+05 (3.6)	1.22E+05 (1.0)
Na (mmol/g)	3.07 (34) ^a	3.51 (3.4)	4.03 (4.0)
Ratio	Average Molar Ratio (%RSD)		
Ti/Zr	2.70 (4.0)	2.88 (2.3)	2.93 (2.4)
Ti/Nb	2.46 (0.17)	2.49 (2.9)	2.50 (1.7)
Zr/Nb	0.95 (0.89)	0.87 (3.0)	0.86 (0.45)
Na/Ti	0.93 (32)	1.08 (1.9)	1.19 (1.3)

^a Average of two sets of duplicate samples with very different results (set #1 avg. 2.17 mmol/g; set #2 avg. 3.98 mmol/g)

9120-B bottom column sub-sample than for the top. The results indicate that alkaline earth metals (Be, Mg, Ca, Sr, and Ba) sorbed to or precipitated on the CST media, even though these species were present at trace levels or were below detectable levels in the simulant feed solution. The pretreated CST also contains some of these elements [16, 17]. The calcium in the upper column sub-samples ranged from 0.07 to 0.18 mmol g dry CST, while the concentrations in the standards ranged from 0.01 to 0.07 mmol/g dry CST. Magnesium loading levels in the column sub-samples were comparable to those in the standards (range for both 0.006 to 0.02 mmol/g dry CST). The alkali metals (Li⁺, K⁺, and Cs⁺) were expected (since they are Group 1 cations) and observed to load onto CST, with the exception of rubidium (Na⁺ was loaded onto the CST prior to column testing). The transition metals iron, manganese, and lead were concentrated on the CST media even though they were present at low or below detectable levels in the simulant feed solution. Iron and lead loading onto CST from waste supernate samples has been observed previously [18]. Iron loading on the upper column sub-samples ranged from 0.02 to 0.03 mmol/g dry CST versus the CST standards which ranged from 0.002 to 0.007 mmol g/dry CST [16, 17]. Aluminum is typically observed in digested CST standard blanks and samples contacted with waste supernate and is likely present due to the presence of some residual simulant. As mentioned above, hafnium is likely a contaminant in the CST. Tantalum is also likely a contaminant associated with the niobium in the CST (both metals in Group 5 of the Periodic Table).

Metal loading data on a mmol/g dry CST basis is provided in Table 3-9 for selected species on the column CST sub-samples. The sodium loading levels for the samples varied for some unknown reason between the top portion of the IE-911 column (3.3 mmol Na⁺/g dry CST) and the remaining samples (4.3-4.6 mmol Na⁺/g dry CST). Correction of the sodium loading values for the digestion standards in Table 3-8 using the F-factor data in Table 2-3 gives the following standard loading values for dry CST: 3.7 mmol Na⁺/g dry CST for IE-911, 4.3 mmol Na⁺/g dry CST for 9120-B, and 4.8 mmol Na⁺/g dry CST for 9140-B. Comparison of the sodium loading levels for the column sub-samples to those for the standards (on the same basis) indicates that the column results are in the same range as the standards and exhibit similar variability and trends. IE-911 CST may have a lower sodium content than the other batches, though the %RSD for the IE-911 standard data was high.

Cesium loading levels ranged from 0.049 to 0.065 mmol Cs⁺/g dry CST for the top portions of the CST beds where cesium saturation is expected. A lower cesium loading (0.037 mmol Cs⁺/g dry CST) was observed for the bottom of the 9120-B CST bed since this portion of the bed was not saturated in cesium (<100% Cs⁺ breakthrough from column). Based on the column breakthrough profiles and modeling, the highest cesium loading was expected for the IE-911 CST column. The calculated dilution factor for IE-911 based on the cesium breakthrough profile (Figure 3-10) was

Table 3-9. Metal Loading Data on the CST Column Sub-Samples.

Metal Loading	IE-911 CST Bed <u>Top</u>	9120-B CST Bed <u>Top</u>	9120-B CST Bed <u>Bottom</u>	9140-B CST Bed <u>Top</u>
	mmol/g dry CST			
Na	3.3	4.6	4.5	4.3
K	0.083	0.077	0.082	0.079
Cs	0.055	0.049	0.037	0.065
Al	0.125	0.145	0.160	0.142
Mg	0.006	0.010	0.011	0.009
Ca	0.070	0.168	0.025	0.180
Sr	0.002	0.005	<2E-04	0.004
Ba	0.003	0.006	<7E-05	0.005
Fe	0.022	0.025	0.017	0.021

0.757, which corresponds to 0.054 mmol Cs⁺/g dry CST (DF multiplied by ZAM-calculated powder maximum loading of 0.07083 mmol Cs⁺/g dry CST) versus the measured value of 0.055 mmol/g CST. The calculated DF for 9140-B CST was 0.616 (Figure 3-10), which corresponds to 0.044 mmol Cs⁺/g dry CST. A similar loading was expected for the 9120-B CST, based on the similarities of the cesium breakthrough profiles. The measured value for the upper portion of the 9120-B CST column of 0.049 mmol Cs⁺/g CST was similar to the predicted value. However, the measured cesium loading for the 9140-B CST of 0.065 mmol Cs⁺/g CST was significantly higher than the calculated value. The measured cesium loading levels for the IE-911 and R9120-B columns were consistent with the cesium breakthrough performance and the ZAM calculations.

It should be noted that the hydraulic testing was conducted on all three columns with the same ~1.5 L of simulant feed solution which initially contained cesium. The R9140-B CST column was evaluated first, so this column was expected to load some additional cesium. However, the amount of cesium in this simulant volume was small (~3.8%) relative to the amount already processed through the column. In addition, processing additional simulant would not result in additional cesium loading on the upper portion of the column, since this portion of the bed should have already been saturated in cesium. Likewise, 0.40 L of additional simulant was processed through the R9120-B CST column beyond the volume processed in Table 2-6, but the amount of additional cesium loaded on the column should not impact the cesium loading on the upper portion of the column. Finally, all three columns were stored in simulant for several weeks at ambient temperature prior to analysis, but the volume of simulant (~1 BV or 25 mL) and the amount of cesium that the CST was exposed to during storage were negligible and should not impact the cesium loading levels on the upper portions of the CST beds. The data also indicates that several

metals besides the alkali metals load onto the CST at levels similar to cesium including calcium and iron. Calcium loading was higher than cesium for all of the upper CST bed sub-samples.

Comparison of the three standard batches of CST shows that they are similar in composition, as expected (Table 3-8). The dilution factor used to convert the ZAM results from the powder (pure) CST form to the engineered form containing zirconia binder should correlate to the amount of binder present if there are no other factors influencing the CST performance (such as varying levels of binder ion exchange site blockage between CST batches). Therefore, it would be expected that the IE-911 would have the lowest amount of binder (i.e., Zr) when compared to the more recent batches, based on the higher Cs loadings observed for IE-911. However, examining the ratios it appears that IE-911 has a slightly higher Zr content when compared to 9120-B and 9140-B as evidenced by the lower Ti/Zr and higher Zr/Nb ratios. (Note: Based on the zirconium leaching characteristics of CST discussed above, it is possible that differences in the caustic pretreatment methods between batches could also impact these ratios.) Another factor expected to influence the performance of the CST is the amount of Nb substitution in the structure, where substitution of a portion of the Ti with Nb increases selectivity for Cs⁺ from high level waste solutions [19]. However, it appears that all three batches of CST have similar Nb content as evidenced by the similar Ti/Nb ratios. The theoretical formula for CST with 25% substitution of Ti with Nb is $\text{HN}_{\text{a}2}\text{Ti}_{\text{3}}\text{NbSi}_{\text{2}}\text{O}_{\text{14}} \cdot \text{xH}_{\text{2}}\text{O}$, which would give a Ti/Nb molar ratio of 3; therefore, it appears the UOP materials have slightly higher than 25% substitution of Ti with Nb.

Analysis results for the digested solids from the simulant drum and the CST columns are provided in Table 3-10. The samples were submitted for analysis as damp solids with unknown amounts of residual water. Sodium in the samples may be partially due to incomplete washing. Titanium, zirconium, and niobium in the samples isolated from the columns is due to the presence of some residual CST. Aluminum and calcium are dominant species present in the drum solids, with magnesium, iron, and manganese being secondary components and numerous other metals being observed at lower levels. Aluminum is also a dominant component for all CST column sub-samples, though some of the aluminum is likely associated with residual CST. The solids from Column B contained significant calcium and magnesium. Column C solids contained calcium and magnesium at lower levels than Column B. Column A solids did not contain detectable calcium but did contain magnesium. All of the column solids contained some iron and manganese. An X-Ray Diffraction (XRD) scan of the drum solids is provided in Figure 3-16, where it is apparent that the dominant crystalline species is calcium carbonate. Other crystalline species present included hydrated sodium calcium carbonate and sodium carbonate phases and the aluminum hydroxide phases gibbsite and bayerite. Energy Dispersive Spectroscopy (not shown) of the drum solids also confirmed the presence of sodium, aluminum, magnesium, calcium, manganese, and iron.

Based on the additional analysis results, supersaturated concentrations of some metal species are believed to have existed in the simulant solution despite the fact that the simulant had been aged for several weeks prior to testing. This resulted in the co-precipitation of calcium, aluminum, magnesium, manganese, and iron species from solution. Supersaturation at ambient temperature was apparent based on the precipitation observed in the drum, which was stored at ambient temperature. In addition, calcium carbonate (observed by XRD in the drum solids) and magnesium carbonate have retrograde solubility (lower solubility at higher temperature) and precipitation of these species in the columns would be expected due to the simulant temperature increase from ambient to 35 °C that occurred in the column heads. Co-precipitation of various species resulted in the formation of solids within and on the CST beads in the upper portions of the columns. The

precipitation of trace levels of transition metals contributed to the brown color of the solids. The precipitation impacted the cesium loading kinetics (media fouling) on the CST columns resulting in linear breakthrough profiles in the effluent solutions.

Table 3-10. ICP-ES and ICP-MS Data on Digested Solids Isolated from the CST Columns and Simulant Drum After Test Completion.

Metal	Solids from Column A (IE-911)	Solids from Column B (9120-B)	Solids from Column C (9140-B)	Simulant Drum Solids
	µg/g solid (hydration level unknown)			
ICP-ES Data				
Al	2140	3230	4890	34100
Ba	<6.49	17.2	10.8	37.7
Cr	<7.32	<5.36	<4.09	69.2
Ca	<47.4	828	72.5	35000
Fe	107	168	124	993
Mg	650	1335	802	2690
Mn	231	373	265	918
Na	2810	4690	6680	25000
Sr	2.7	8.5	4.2	20.6
Ti	1920	902	887	176
Zn	<9.41	<6.89	<5.58	36.1
Zr	1030	445	425	<35.9
ICP-MS Data				
Sr	2.61	8.22	3.85	20.9
Zr	1080	451	446	33.3
Nb	1540	<15.3	815	78
Cs ⁺	66	35	41	<3.2
Ba	6.9	18.3	11	37
Hf	18	7.8	7.4	<3.2

CST sub-samples from the columns were submitted for Microtrac particle size analysis. The results are provided in Table 3-11 and Figures 3-17 through 3-19. The IE-911 volume-based mean particle diameter determined by Microtrac analysis was near 500 µm and the mean diameters of the 9120-B and 9140-B CST samples were near 600 µm. For comparison, the volume-based mean particle diameters for each CST sample based on vendor sieve data collected during media production are also provided in Table 3-12. The vendor sieve data indicated that the average particle diameter was closer to 400 µm for IE-911 CST. The packed bed drainable volume fractions (reported above) for each media sample are also provided for trend comparison. It should be noted that the drainable void volume fraction data does not include immobile water within the pores of the CST media or trapped between beads due to surface tension.

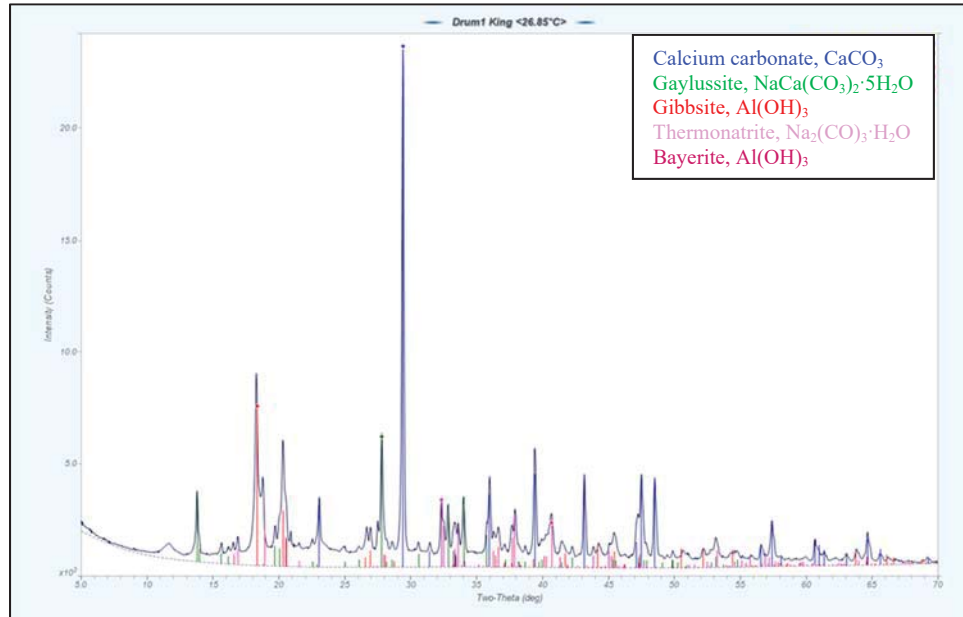


Figure 3-16. X-Ray Diffraction Scan of the Simulant Drum Solids.

Table 3-11. Microtrac Particle Size Distribution Data for CST Column Sub-Samples.

CST	μm				
	Mean Volume	Mean Number	Mean Area	Standard Deviation	50 th Percentile
IE-911	516	447	490	111	494
9120-B	608	515	573	142	584
9140-B	638	533	599	153	614

Table 3-12. Particle Size Distribution and Drainable Void Data for CST Production Batches and Column Sub-Samples.

CST	Volume Based Mean Diameter (μm)		Drainable Volume % ^c
	Vendor Sieve ^a	Microtrac ^b	
IE-911	408	516	18.0
9120-B	583	608	22.9
9140-B	614	638	27.4

^a based on CST production batch data

^b column test bed sub-samples

^c repacked CST beds in water at ambient temperature

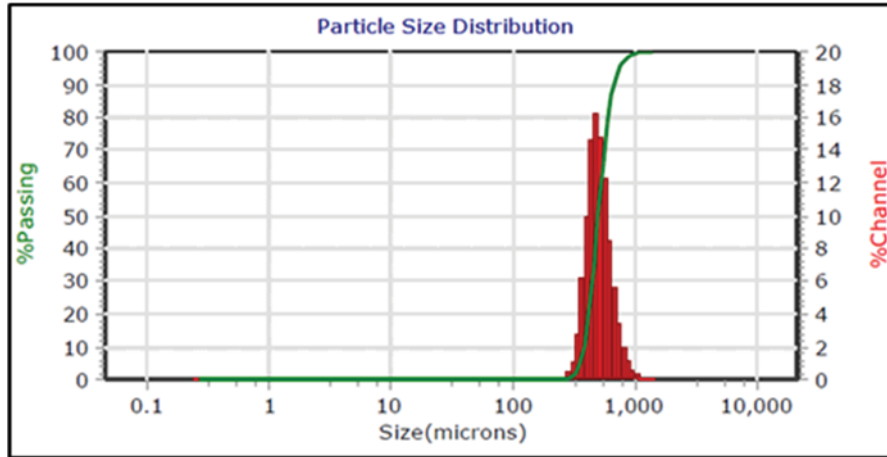


Figure 3-17. Volume-Based Microtrac Particle Size Distribution for the IE-911 CST Sub-sample from Column A.

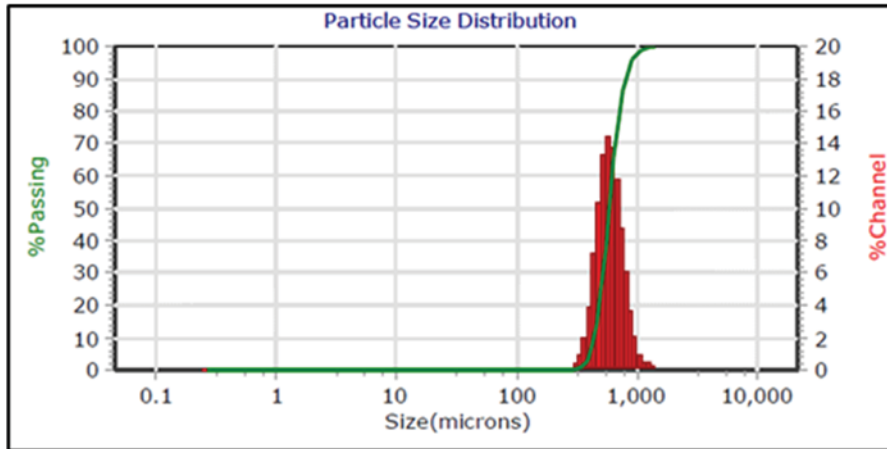


Figure 3-18. Volume-Based Microtrac Particle Size Distribution for the 9120-B CST Sub-sample from Column B.

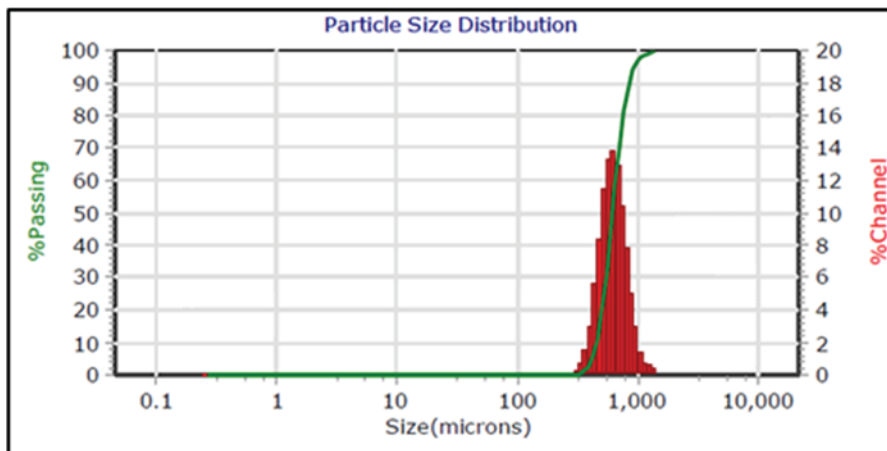


Figure 3-19. Volume-Based Microtrac Particle Size Distribution for the 9140-B CST Sub-sample from Column C.

4.0 Conclusions

Batch contact equilibrium tests with SRS Average Simulant indicated that the archived IE-911 CST batch has a higher cesium capacity than recently prepared batches. The results also indicate that the minor TCCR CST 9120-B media lot (2099000035) has similar cesium removal performance to the major TCCR lot (2099000034). The measured equilibrium distribution coefficients for IE-911 CST in simulant at 25 °C were significantly lower than previous results indicating reduced cesium removal performance with this simulant batch. A ZAM Model DF value of 0.5 was required for the 9120-B and 9140-B batches for predictions to match experimental data while a DF near 0.6 (20% higher) was required for the IE-911 batch at 35 °C. This dilution factor indicated a 26% cesium capacity reduction for the 9140-B CST and a 40% reduction for the IE-911 CST relative to previous test results with the same CST samples, but a different simulant batch. The reason for the low CST performance with this simulant batch is not understood.

Column tests were also conducted with each CST batch and SRS simulant at 35 °C. Nearly linear cesium breakthrough profiles were observed for each column under these conditions. The VERSE model predictions of the cesium column breakthrough profiles for the IE-911 and 9140-B CST columns based on the batch contact results indicated that the observed 50% breakthrough points were later than predicted based on the recent batch contact data with the simulant batch used for column testing, but were significantly sooner than would have been predicted based on historical testing with different simulant batches. Significantly greater (40%) bed volumes of simulant were processed with the IE-911 CST prior to reaching the 50% cesium breakthrough point relative to the other two CST batches. Plotting the breakthrough data versus cumulative simulant volume processed revealed that with equal masses of CST in the columns the 50% breakthrough point for IE-911 CST was only 30% higher than observed with the newer CST batches. The packed bed density of IE-911 CST is 10% higher than the density of 9140-B CST. The combined effects of higher capacity and higher density for IE-911 CST resulted in 40% more column bed volumes processed to reach 50% cesium breakthrough. Additional evaluations revealed that the cesium breakthrough profiles for each column were much less sharp than predicted at this temperature, indicating reduced cesium loading kinetics with this simulant relative to historical results.

The cesium removal performance results are consistent with fouling of the CST media. During the first few hours of column testing, a brown residue was observed to form on the top portion of each CST column. It is possible that fouling of the CST may have occurred, and this may explain the reduced cesium capacity and performance of the media during column testing. Analyses of the simulant batch utilized for testing was as expected with no indication of impurities.

Overall, the results indicate that the media performance for all of the CST batches tested with this simulant batch was reduced relative to previous testing. The column data also indicates reduced cesium loading kinetics relative to recent results with these materials and historical data. Despite the reduced performance associated with this simulant, it is apparent from the data that the IE-911 CST media is superior in performance to the recently-prepared CST batches with regard to cesium loading capacity and density and that significantly greater volumes of waste could be processed for a given column volume relative to more recently prepared batches.

Teabag test results indicated that higher cesium loading is observed with the recently modified, more open teabag design when using a 10-day test duration. The results also showed that while

cesium loads at substantially lower amounts than ZAM predicts, the potassium loadings are in much better agreement with predicted values from ZAM.

Hydraulic testing conducted on each CST column at the conclusion of cesium performance testing revealed linear frictional pressure drop dependence with flow rate indicating laminar flow conditions. The highest pressure drop data was observed with IE-911 CST which had the smallest average particle diameter, while the lowest pressure drop data was observed with the more recently prepared 9140-B CST media. Based on the results, IE-911 CST is expected to have 19% higher pressure drop than the TCCR 9120-B CST under dynamic flow conditions, while the 9140-B CST is expected to have 28% lower pressure drop than 9120-B. Relative to IE-911 CST, 16 and 39% lower pressure drops, respectively, were observed for 9120-B and 9140-B CST samples. The mobile fluid bed volume fractions determined separately for each CST batch are representative of the packed bed porosity and correlate better to the trends in the hydraulic data than the mean particle diameter values.

Additional analysis data in report revision 2 on the simulant, the CST media in the columns, the solids isolated from the simulant drum and columns, and CST blank samples was needed to explain the poor cesium loading kinetics observed for the CST columns. Based on the analysis results, supersaturated concentrations of some metal species are believed to have existed in the simulant solution despite the fact that the simulant had been aged for several weeks prior to testing. This resulted in the co-precipitation of calcium, aluminum, magnesium, manganese, and iron species from solution. Except for aluminum, the metals were present at concentrations below analytical detection limits in the column simulant feed. These species included calcium carbonate and possibly magnesium carbonate, which have retrograde solubility and would be expected to have precipitated in the column head when the temperature was increased from ambient to 35 °C. Co-precipitation of various species resulted in the formation of small amounts of solids within and on the CST beads in the upper portions of the columns. The precipitation of trace levels of transition metals contributed to the brown color of the solids. The precipitation impacted the cesium loading kinetics on the CST columns resulting in linear breakthrough profiles in the effluent solutions. Measured cesium loading levels for two of the three CST columns were consistent with ZAM-calculated loading values based on the cesium breakthrough profiles (higher loading for the third column was not understood).

5.0 Recommendations and Path Forward

Simulant cesium loading kinetics and capacity evaluations of new CST production batches prepared for use in the next TCCR columns will be needed to understand and predict the performance of the new columns. The new CST batches and individual lots should be pretreated and characterized following the methods and protocols developed previously. Model performance predictions should be conducted for the new TCCR columns based on the simulant data, CST characterization, and Tank 9/10 batch contact results.

It is recommended that the more open teabag holder design be utilized for future teabag batch contacts in the field. Simulant teabag testing is recommended using the new CST batch prior to field teabag implementation.

Based on the additional data collected and reported in report revision 2, future simulant preparations should involve aging and filtering the simulant at test temperature to avoid precipitation of trace supersaturated metals which can form solids in large simulant batches at sufficient quantities to promote CST fouling. Although it has been used for testing for many years,

the SRS average simulant appears to be supersaturated in aluminum. Recipe modifications should be considered for future preparations and applications of this simulant. As observed in other recent tests, CST has again been shown to have a propensity for fouling or being otherwise impacted with regard to cesium removal performance by the presence of certain alkaline earth or transition metals at low levels. Further study of this phenomenon is recommended.

6.0 References

1. W. D. King, L. L. Hamm, D. J. McCabe, C. A. Nash, F. F. Fondeur, "Crystalline Silicotitanate Ion Exchange Media Long-Term Storage Evaluation", SRNL-STI-2018-00567, Rev. 0, November 2018.
2. W. D. King, L. L. Hamm, C. J. Coleman, F. F. Fondeur, S. H. Reboul, "Crystalline Silicotitanate (CST) Ion Exchange Media Performance Evaluations in SRS Average Supernate Simulant and Tank 10H Waste Solution to Support TCCR", SRNL-STI-2018-00277, Rev. 0, June 2018.
3. C. A. Nash, T. Hang, "Stagnant and Stirred 10-Day Teabag Test Supporting Tank Closure Cesium Removal", SRNL-L3160-2019-00001, Rev. 0, May 13, 2019.
4. W. D. King, D. J. McCabe, C. A. Nash, "Task Technical and Quality Assurance Plan for CST Batch Contact and Column Testing to Support Tank Closure Cesium Removal Operations", SRNL-RP-2019-00350, Rev. 1, July 2019.
5. T. L. Fellingner, "Research and Development (R&D) for Tank 9 Processing Through the Tank Closure Cesium Removal (TCCR) Unit", X-TTR-H-00085, Rev. 0, May 2019.
6. D. A. Tamburello, "Software Classification Document – ZAM," B-SWCD-A-00598, May 2011.
7. L. L. Hamm, T. Hang, D. J. McCabe, and W. D. King, "Preliminary Ion Exchange Modeling for Removal of Cesium from Hanford Waste Using Hydrous Crystalline Silicotitanate Material," WSRC-TR-2001-00400, SRT-RPP-2001-00134, Rev. 0, 2002.
8. Hamm, L. L., F. G. Smith, and M. A. Shadday, 1999. "QA Verification Package for VERSE-LC Version 7.80," WSRC-TR-99-00238, Rev. 0.
9. T. Hang, "Software Classification Document – VERSE-LC," G-SWCD-A-00060, Rev. 0, 2017.
10. K. M. L. Taylor-Pashow, T. B. Edwards, C. A. Nash, "Pretreatment of Crystalline Silicotitanate (CST) and Development of a Digestion Standard to Support Tank Closure Cesium Removal (TCCR)", SRNL-STI-2019-00045, Rev. 0, March 2019.
11. Walker, D. D., "Preparation of Simulated Waste Solutions", WSRC-TR-99-00116, Rev. 0, April 1999.
12. K. M. L. Taylor-Pashow, T. Hang, C. A. Nash, "Summary of Expedited Results from Samples Supporting Tank Closure Cesium Removal (TCCR) Batch 1A and Modeling Results for Cs Loading on CST", SRNL-L3100-2019-00002, Rev. 2, February 19, 2019.

13. Manual L29, Procedure ITS-0230, Rev. 0, "Receipt and Preparation of Samples from In-Tank Batch Contact Testing", effective October 18, 2018.
14. Z. Zheng, R. G. Anthony, J. E. Miller, "Modeling Multicomponent Ion Exchange Equilibrium Utilizing Hydrous Crystalline Solicitants by a Multiple Interactive Ion Exchange Site Model", *Ind. Eng. Chem. Res.*, 1997, Vol. 36, No. 6, pp. 2427-2434.
15. K. Gotoh, H., Masuda, K. Higashitani, "Powder Technology Handbook", 2nd Revised Edition, Marcel Dekker, New York, 1997.
16. W. D. King, K. M. Taylor-Pashow, T. Hang, F. F. Fondeur, "Characterization and CST Batch Contact Equilibrium Testing of Aged TCCR Tank 10H Batch 1A and 2 Process Supernate Samples", SRNL-STI-2019-00623, Rev. 0, October 2019.
17. K. M. L. Taylor-Pashow, W. D. King, T. Hang, F. F. Fondeur, "Characterization and CST Batch Contact Equilibrium Testing of Modified Tank 9H Process Supernate Samples in Support of TCCR", SRNL-STI-2020-00128, Rev. 0, April 2020.
18. K. M. L. Taylor-Pashow, T. Hang, C. A. Nash, "Summary of Expedited Results from Samples Supporting Tank Closure Cesium Removal (TCCR) Batch 2 and Modeling Results for Cs Loading on CST", SRNL-L3100-2019-00017, Rev. 0, May 21, 2019.
19. A. Tripathi, D. G. Medvedev, M. Nyman, and A. Clearfield, "Selectivity for Cs and Sr in Nb-substituted Titanosilicate with Sitenakite Topology" *J. Solid State Chem.*, 2003, 175, 72-83.

Appendix A. TGA Data

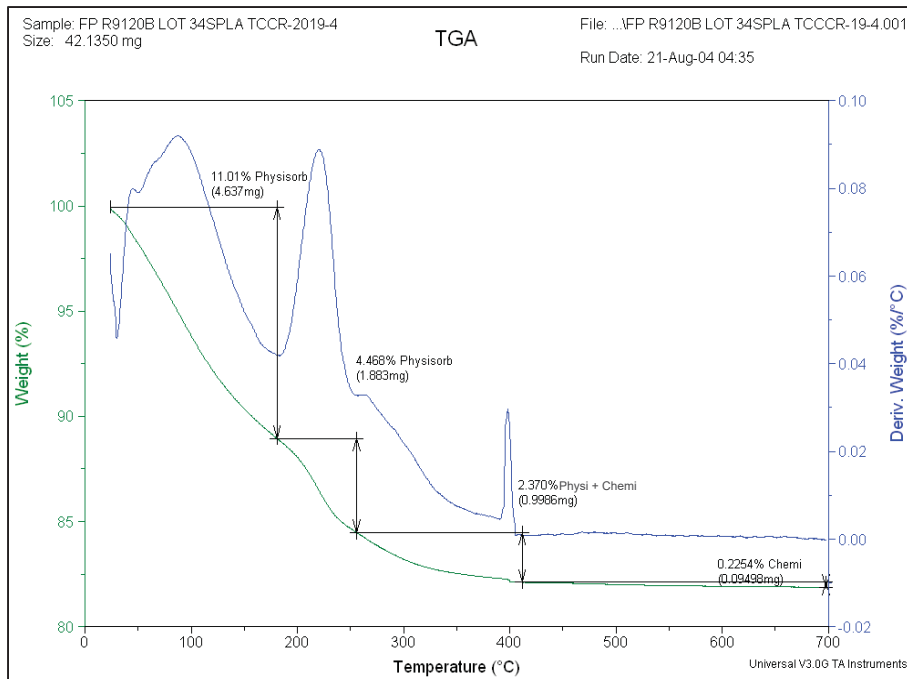


Figure A-1. TGA Mass Loss Profiles versus Time for Field-Pretreated CST Batch 9120-B Lot #2099000034 Sample A.

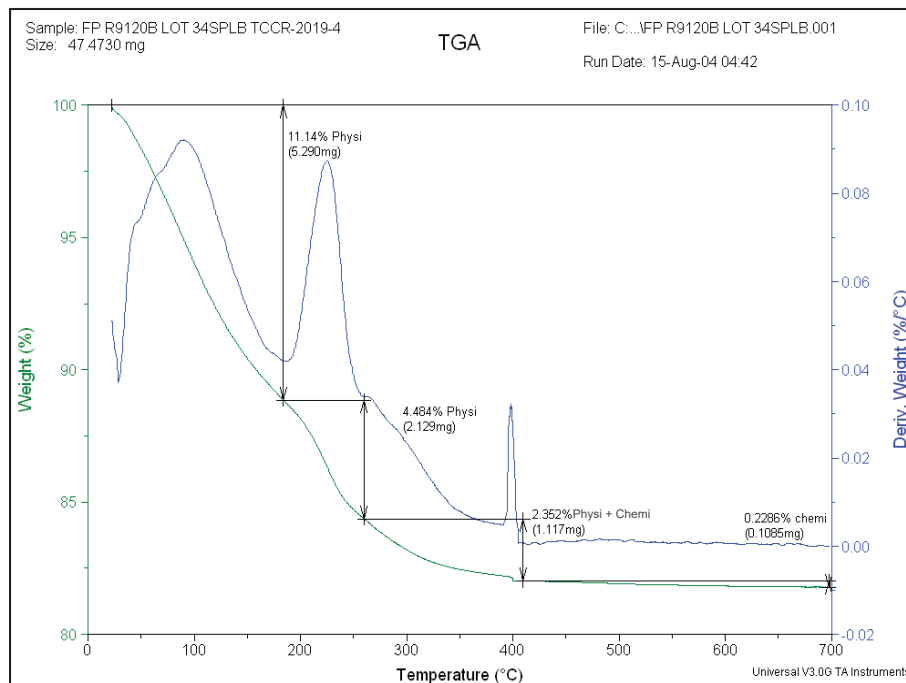


Figure A-2. TGA Mass Loss Profiles versus Time for Field-Pretreated CST Batch 9120-B Lot #2099000034 Sample B.

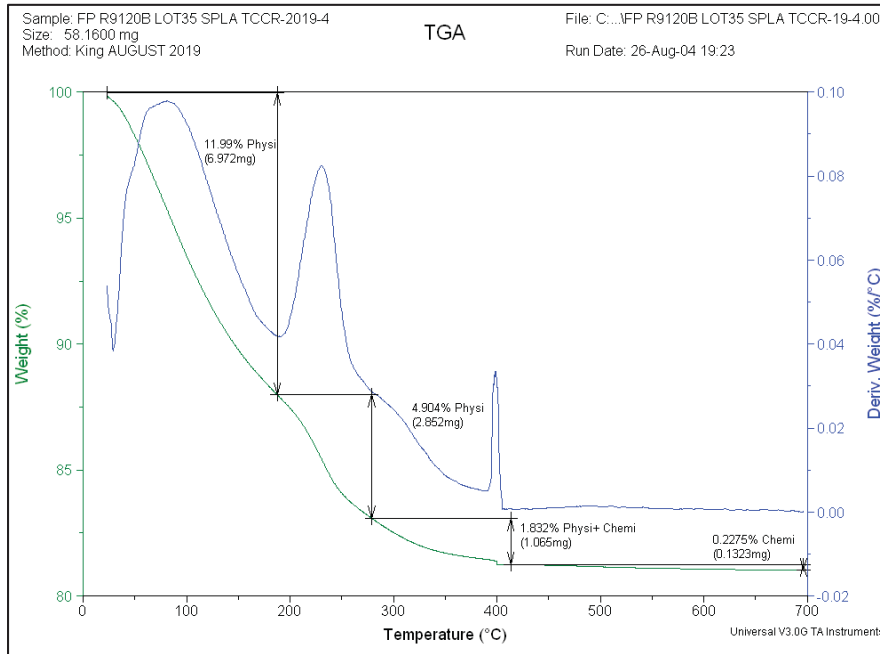


Figure A-3. TGA Mass Loss Profiles versus Time for Field-Pretreated CST Batch 9120-B Lot #2099000035 Sample A.

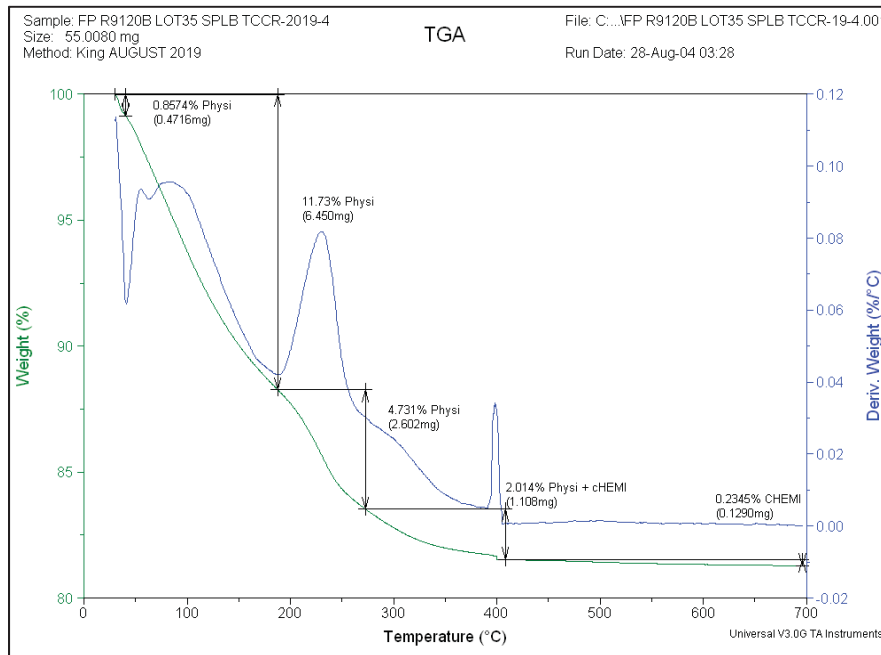


Figure A-4. TGA Mass Loss Profiles versus Time for Field-Pretreated CST Batch 9120-B Lot #2099000035 Sample B.

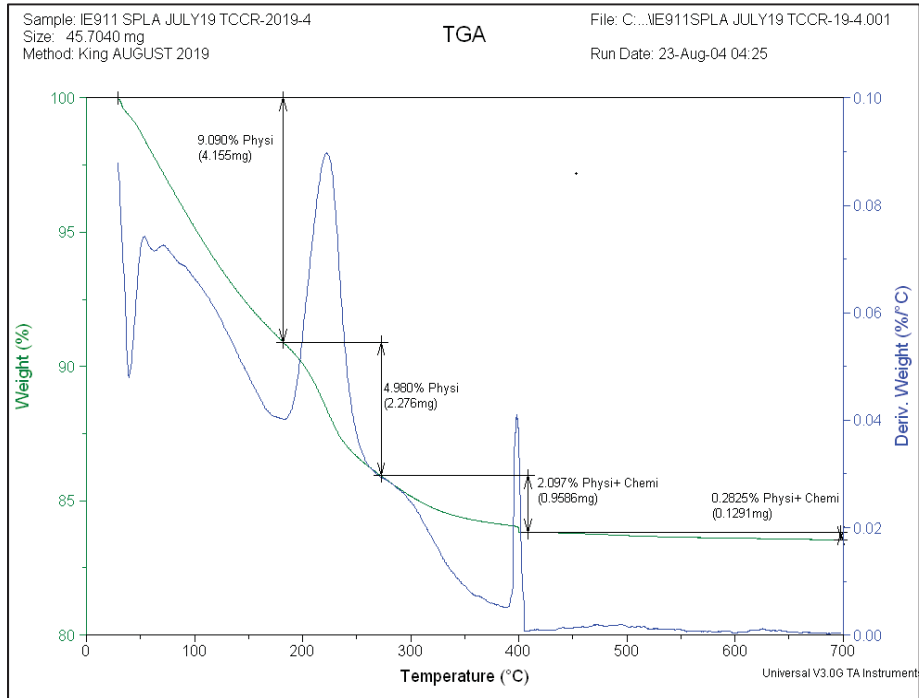


Figure A-5. TGA Mass Loss Profiles versus Time for Vendor-Pretreated CST Batch IE-911 Sample A.

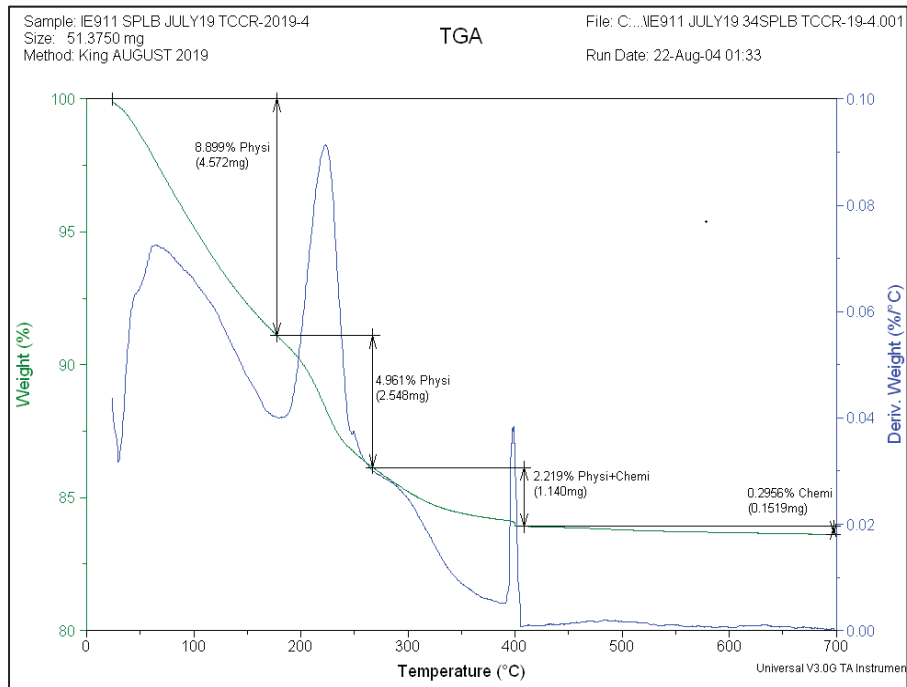


Figure A-6. TGA Mass Loss Profiles versus Time for Vendor-Pretreated CST Batch IE-911 Sample B.

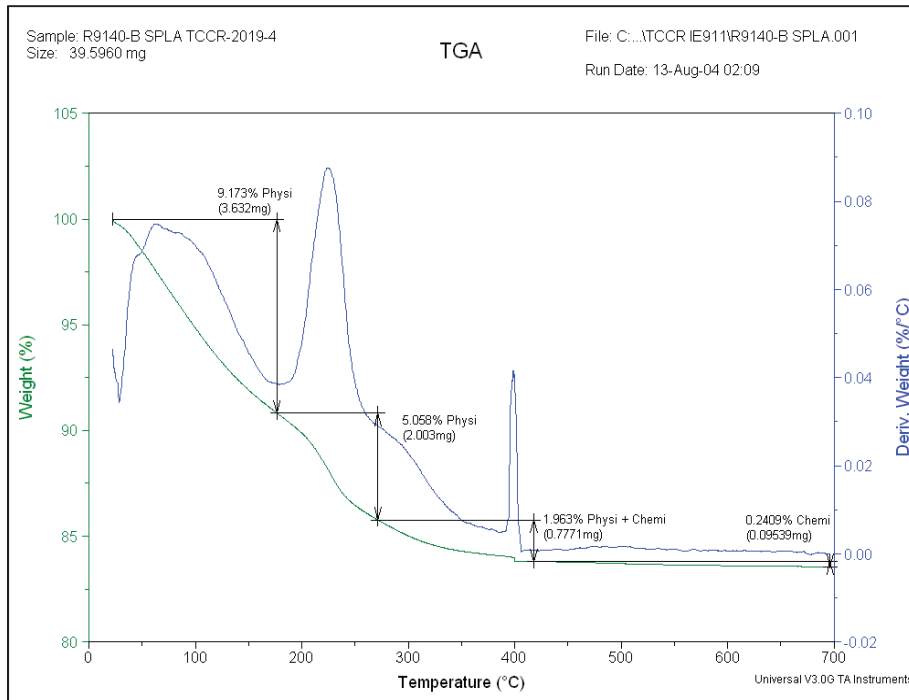


Figure A-7. TGA Mass Loss Profiles versus Time for Vendor-Pretreated CST Batch 9140-B Sample A.

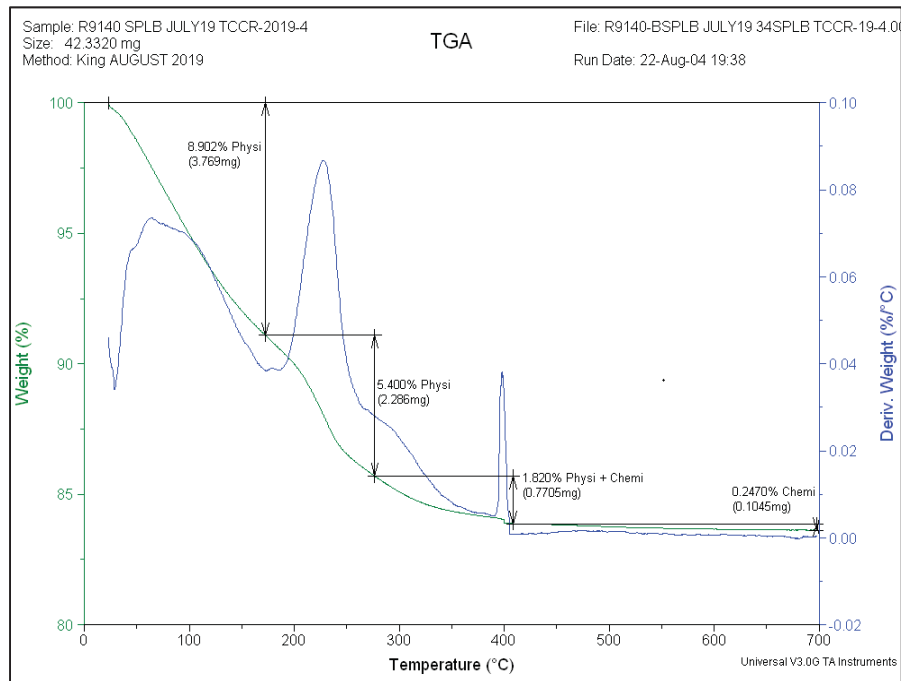


Figure A-8. TGA Mass Loss Profiles versus Time for Vendor-Pretreated CST Batch 9140-B Sample B

Appendix B. ZAM β Factor Temperature Dependence for SRS Average Simulant.

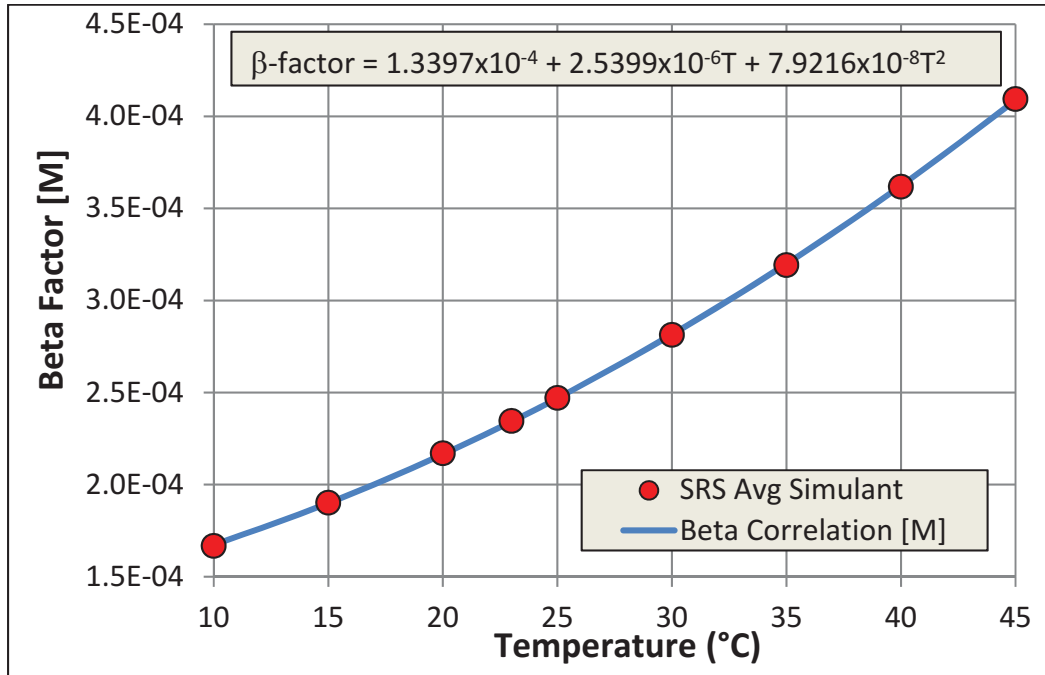


Figure B-1. ZAM β Factor Temperature Dependence for SRS Average Simulant.

Table B-1. SRS Average Simulant ZAM β Factors for Various Temperatures.

Temp. (°C)	β Parameter (M)
10	1.667E-04
15	1.902E-04
20	2.170E-04
23	2.346E-04
25	2.471E-04
30	2.813E-04
35	3.192E-04
40	3.618E-04
45	4.094E-04

Appendix C. Teabag CST Digestion Data.

Table C-1. Analysis Results for Selected CST Components from the Digested Media Samples from Teabag Test A.

Component	Wt. %		
	Test A Carboy 1	Test A Carboy 2	Control
Ti	13.2	14.8	15.3
Nb	10.3	11.4	12.0
Zr	8.83	9.71	10.3
Na	10.6	8.70	8.15

Table C-2. Analysis Results for Selected CST Components from the Digested Media Samples from Teabag Test B.

Component	Wt. %		
	Test B Carboy 1	Test B Carboy 2	Control
Ti	13.0	12.6	15.4
Nb	9.75	9.49	11.9
Zr	8.48	8.18	10.3
Na	9.15	9.84	7.79

Table C-3. Analysis Results for Cs⁺ and K⁺ on Teabag CST Samples.

Test	Species	μg/g on CST	Total μg	K _d , mL/g ^a
1A	Cs ⁺	536	52.8	115
	K ⁺	3060		
2A	Cs ⁺	2490	252	535
	K ⁺	3560		
1B	Cs ⁺	1830	205	396
	K ⁺	2660		
2B	Cs ⁺	2200	268	476
	K ⁺	2700		

^a dry, engineered CST mass basis

Table C-4. Analysis Results for Other Selected Sorbed Species (Ca⁺² and Fe⁺³) on Teabag CST Samples

Test	Liquid Phase	Species	µg/g on CST*	µg/g on CST Standard*	Ratio (sample/standard)
1A	SRS Average Simulant	Ca ⁺²	910	971	0.94
		Fe ⁺³	832	216	3.9
2A		Ca ⁺²	1180	971	1.2
		Fe ⁺³	1190	216	5.5
1B		Ca ⁺²	1400	809	1.7
		Fe ⁺³	594	241	2.5
2B		Ca ⁺²	896	809	1.1
		Fe ⁺³	737	241	3.1
Batch 1A**	Tank 10H	Ca ⁺²	3350	1110	3.0
		Fe ⁺³	1500	342	4.4

*Not adjusted for DF or F Factor

** Reference 12

Distribution:

alex.cozzi@srnl.doe.gov
david.crowley@srnl.doe.gov
a.fellinger@srnl.doe.gov
samuel.fink@srnl.doe.gov
joseph.manna@srnl.doe.gov
gregg.morgan@srnl.doe.gov
john.mayer@srnl.doe.gov
erich.hansen@srnl.doe.gov
connie.herman@srnl.doe.gov
daniel.mccabe@srnl.doe.gov
Boyd.Wiedenman@srnl.doe.gov
chris.martino@srnl.doe.gov
william02king@srnl.doe.gov
richard.wyrwas@srnl.doe.gov
michael.stone@srnl.doe.gov
luther.hamm@srnl.doe.gov
charles.nash@srnl.doe.gov
amy.ramsey@srnl.doe.gov
kathryn.taylor-pashow@srnl.doe.gov
eric.freed@srs.gov
richard.edwards@srs.gov
vijay.Jain@srs.gov
tony.polk@srs.gov
patricia.suggs@srs.gov
terri.fellinger@srs.gov
Aubrey.Silker@srs.gov
Alexander.Luzzatti@srs.gov
david02.martin@srs.gov
john.occhipinti@srs.gov
john.iaukea@srs.gov
Rachel.Seeley@srs.gov
gregory.arthur@srs.gov
Records Administration (EDWS)